JOURNAL OF GEOPHYSICAL RESEARCH, VOL. 113, A08102, doi:10.1029/2007JA012920, 2008

Interplanetary coronal mass ejections that are undetected by solar coronagraphs

T. A. Howard[1] and G. M. Simnett[2]

Received 2 November 2007; revised 17 March 2008; accepted 27 March 2008; published 2 August 2008.

[1] From February 2003 to September 2005 the Solar Mass Ejection Imager on the Coriolis spacecraft detected 207 interplanetary coronal mass ejections (ICME) in the inner heliosphere. We have examined the data from the Large Angle Spectroscopic Coronagraph (LASCO) on the SOHO spacecraft for evidence of coronal transient activity that might have been the solar progenitor of the Solar Mass Ejection Imager (SMEI) events, taking into account the projected speed of the SMEI event and its position angle in the plane of the sky. We found a significant number of SMEI events where there is either only a weak or unlikely coronal mass ejection (CME) detected by LASCO or no event at all. A discussion of the effects of projection across large distances on the ICME measurements is made, along with a new technique called the Cube-Fit procedure that was designed to model the ICME trajectory more accurately than simple linear fits to elongation-time plots. Of the 207 SMEI events, 189 occurred during periods of full LASCO data coverage. Of these, 32 or 17% were found to have a weak or unlikely LASCO counterpart, and 14 or 7% had no apparent LASCO transient association. Using solar X-ray, EUV and Hα data we investigated three main physical possibilities for ICME occurrence with no LASCO counterpart: (1) Corotating interaction regions (CIRs), (2) erupting magnetic structures (EMS), and (3) flare blast waves. We find that only one event may possibly be a CIR and that flare blast waves can be ruled out. The most likely phenomenon is investigated and discussed, that of EMS. Here, the transient erupts in the same manner as a typical CME, except that they do not have sufficient mass to be detected by LASCO. As the structure moves outward, it accumulates and concentrates solar wind material until it is bright enough to be detected by SMEI.

Citation: Howard, T. A., and G. M. Simnett (2008), Interplanetary coronal mass ejections that are undetected by solar coronagraphs, *J. Geophys. Res.*, *113*, A08102, doi:10.1029/2007JA012920.

1. Introduction

[2] Coronal mass ejections (CMEs) are an important mechanism removing large amounts of energy and magnetic helicity from the Sun. They are also of interest because their impact with the Earth may cause geomagnetic storms, that can result in severe space weather effects. Physically CMEs are density enhancements of coronal plasma that have frozen-in magnetic fields, of size that may span several tens of degrees of heliospheric latitude and masses that may exceed 10^{13} kg. Early in their evolution out to 0.1–0.2 AU they may achieve speeds greater than 3000 km/s.

[3] Close to the Sun, CMEs are generally detected using coronagraphs, that block out the majority of the light from the Sun with an occulting disk, revealing the faint surrounding corona. The most successful coronagraph to date for CME detection is the Large Angle Spectroscopic Coronagraph (LASCO) [*Brueckner et al.*, 1995]. During its 12 years of operation LASCO has detected well over 10^4 CMEs, many of which have been documented in various online catalogs [e.g., *St. Cyr et al.*, 2000; *Yashiro et al.*, 2004]. Beyond the fields of view of coronagraphs, the only means of detecting CMEs until recently was either in situ, using spacecraft in the solar wind such as ACE, WIND and Ulysses, or by fluctuations in the meter wavelength radio spectrum caused by the passage of a CME. This is called interplanetary scintillation [*Hewish et al.*, 1964]. Radio bursts driven by CME-induced shocks also provide information on interplanetary CME, or ICME [*Zhao*, 1992] propagation. These are known as type II radio bursts [*Wild et al.*, 1963]. Historically ICME detection was therefore limited to those that passed directly by the in situ spacecraft (i.e., Earth-directed) and those most favored for radio detection. More recently the Solar Mass Ejection Imager (SMEI) [*Eyles et al.*, 2003; *Jackson et al.*, 2004] has provided direct imaging of ICMEs from around 20° elongation out to beyond 1 AU. From the start of operation in February 2003 until the end of 2007, it has detected and tracked around 300 ICMEs.

[1] Air Force Research Laboratory, Space Vehicles Directorate, Sunspot, New Mexico, USA.
[2] School of Physics and Astronomy, University of Birmingham, Edgbaston, UK.

0148-0227/08/2007JA012920$09.00

[4] One discovery which has emerged using these various instruments and techniques is that some ICMEs occur where no associated CME has been observed in LASCO [*Simnett*, 2005]. *Cane and Richardson* [2003] conducted a survey of magnetic clouds and interplanetary shocks detected with ACE and WIND across a 6-year time period, and found that around half of their events were probably not associated with halo or partial halo CMEs. Halo CMEs, or HCMEs are CMEs that have a major component along the Sun-Earth line, and so appear in coronagraphs as sky-plane-projected halos that encircle the occulting disk and expand outward [*Howard et al.*, 1982]. Partial halo CMEs have an apparent width greater than around 120° position angle, and are therefore also likely to have a large component directed along the Sun-Earth line. *Schwenn et al.* [2005] identified eight interplanetary transients that they claimed were not associated with HCMEs, although four of these were later revealed to be associated [*Howard and Tappin*, 2005b]. *Howard and Tappin* [2005a] identified seven interplanetary shocks out of almost 300 across an 8 year time period for which no halo, or partial halo CME could be associated. They later conducted an investigation of these seven events [*Howard and Tappin*, 2005b] and found that five could not be described as corotating interaction regions [*Smith and Wolfe*, 1976] either. They concluded that the CMEs did in fact originate from the Sun and the physics driving them were identical to those driving typical CMEs, except that they did not contain sufficient plasma to be detected by coronagraphs. *Shanmugaraju et al.* [2006] identified 30 events out of around 400 metric Type II radio bursts across almost 4 years for which there were no CMEs in LASCO reported. *Tripathi et al.* [2004] reported a close association between posteruptive arcades and CMEs and found that 19 out of 229, or 7% were not associated with a CME.

[5] Unlike the other instruments, SMEI is not restricted to those events that are Earth-directed, and it has detected several ICMEs that have not been associated with CMEs in LASCO. Preliminary results reported by *Simnett* [2005] found that around 15% of SMEI events were not associated with LASCO CME activity at all, and that a further 10% only had a weak association with activity detected by LASCO. He suggested that if the CME at LASCO was responsible for the ICME in SMEI then the physics behind its evolution must extend beyond simple MHD propagation.

[6] It is the objective of the present study to conduct an investigation of SMEI ICMEs that are not directly associated with LASCO CMEs, and identify which of the mechanisms discussed above is/are responsible for their occurrence. We investigate three following possibilities: (1) Corotating interaction regions, (2) Erupting magnetic structures, and (3) Flare blast waves. It was found that 7% of the SMEI ICMEs were not associated with any activity in LASCO, with a further 17% associated with very weak LASCO activity. A discussion of the physical implications ensues.

2. Data

[7] The primary database for our work is provided by SMEI on board the Coriolis spacecraft. SMEI images the entire sky in white light beyond 20° elongation, and most of the events to date have been detected within 1 AU. Each all-sky image is acquired during the spacecraft's 102 min polar orbit. The SMEI database begins in February 2003 and continues to the present. Coronagraph comparisons with the SMEI ICME events were made using LASCO on board the SOHO spacecraft. We have used the LASCO/C2 coronagraph, that has a field-of-view of 1.5–6 $R_\odot$ and a cadence of around 30 min, and the LASCO/C3 coronagraph with a field-of-view of 3.7–30 $R_\odot$ and cadence of around 50 min. We have examined the running difference images from LASCO at high contrast and sensitivity levels to try and identify the faintest events possible that might have resulted in an event detected by SMEI.

[8] As SMEI is an all-sky camera, its images are Hammer-Aitoff projected [*Leighly*, 1955], and as such are projected into the two-dimensional sky plane. Distance measurements are made in units of elongation angle ϵ, where ϵ is the angle between the Sun-Earth line and the line between the Earth and the point being measured. For a CME heading directly toward the Earth an elongation of 90° is the location of the Earth and 180° is directly behind the Earth as it faces the Sun, or the local midnight meridian. A report dealing with the conversion of large elongation angles to units of distance is given by *Howard et al.* [2007]. This paper also includes two examples of SMEI images with ICMEs that are associated with LASCO CMEs.

[9] For comparison with solar phenomena, we have utilized X-ray data from the GOES network and Soft X-ray Imager (SXI) data from GOES-12. Ground-based Hα solar telescope data were also employed. X-ray and Hα flares have been cataloged extensively for decades and these databases are made available via the NOAA/SEC Solar Geophysical Database (US Dept. of Commerce). We have also utilized solar EUV data, provided by the Extreme-Ultraviolet Imaging Telescope (EIT) [*Delaboudinière et al.*, 1995] on board SOHO. Only images from the Fe XII 195 Å line (which is the dominant EUV emission line from plasma at a temperature of $\sim 1.5 \times 10^6$ K) have been used in the present study. Full-disk solar images in this wavelength band typically have a cadence of around 12 min.

3. Event Selection and Analysis

3.1. Events

[10] During the 32 month time period from February 2003 to September 2005, the SMEI team has identified and tracked 207 interplanetary transients. In previous papers dealing with the identification of SMEI ICME onset times [e.g., *Simnett*, 2005], a linear fit was made through the data and this fit extrapolated back to $\epsilon = 0$. For many events, and for a first order approximation such a fit is generally suitable. However, it must be noted that elongation-time evolution is heavily dependent on not only the speed with which the ICME is traveling, but also its direction. Figure 1 shows the range of elongation-time plots for a single point traveling at 1000 km/s. Each curve is the result of different longitudes, from near the Sun-Earth line (solar disk center) to the solar limb, and each panel represents the same range of plots at different latitudes from the equator to the pole. Despite the fact that the speed of the point is constant, in no case is there a linear relationship between elongation and time. For those events closer to the solar limb, a linear fit would seem to be reasonable but this is not true for those events near the Sun-Earth line.

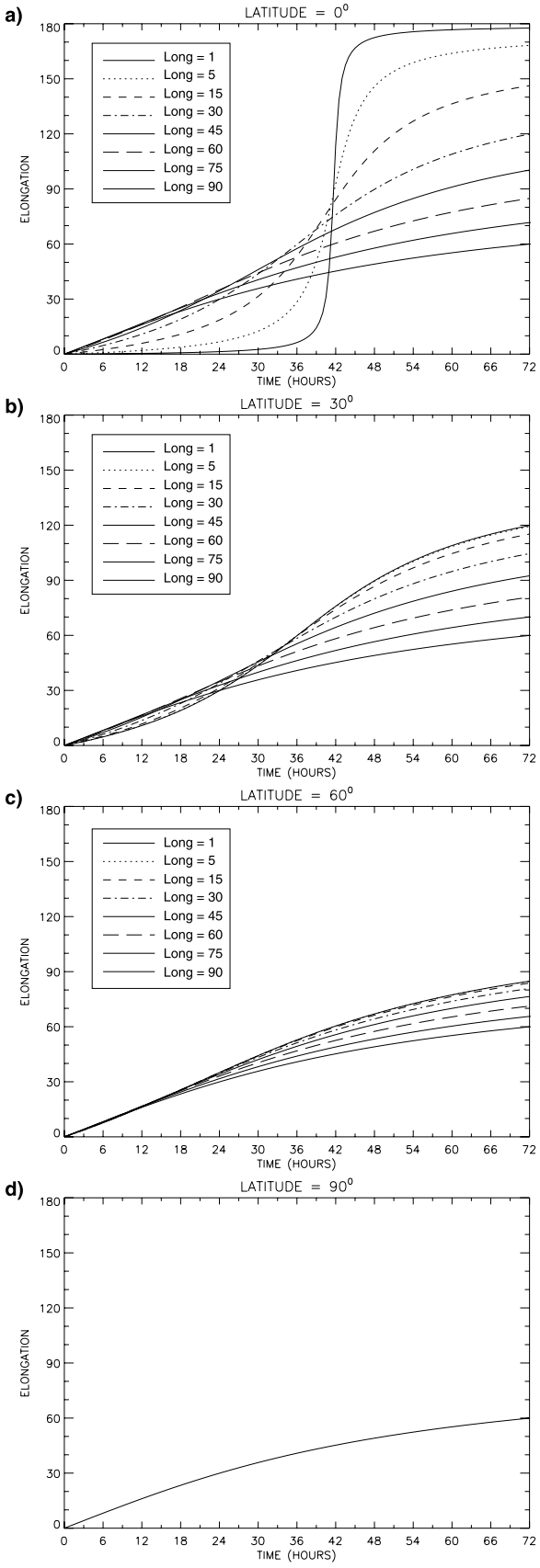

Figure 1. Elongation-time plots for a single point traveling with constant speed (1000 km/s) in different directions. We assume the point is launched at time $t = 0$. The curves shown here represent the appearance of the elongation-time plot for the same points traveling (a) in the equatorial plane (latitude = 0°), and latitudes of (b) 30°, (c) 60°, and (d) 90° (directly north or south). The curves shown are for longitudes of 1°, 5°, 15°, 30°, 45°, 60°, 75°, and 90°. 0° longitude represents the Sun-Earth line, or solar disk center and 90° represents the solar limb.

[11] It should also be noted that for the point traveling in the equatorial plane near the Sun-Earth line (longitude = 1°), the curve reaches $\epsilon = 90°$ just under 42 h after launch. This corresponds to the time for a 1000 km/s CME to travel a distance of 1 AU (41 h, 40 min). As we move closer to the limb and further from the equator it takes longer for the same CME to reach 90° elongation. This is because of the effects of converting an all-sky image to a Hammer-Aitoff projection, and consequently at the solar limb an elongation of 90° no longer indicates a distance of 1 AU from the Sun. The theory behind the conversion of elongation to distance using the direction of propagation has been discussed by *Howard et al.* [2007].

[12] The simple example shown in Figure 1 demonstrates the need to utilize proper elongation-time curves to estimate the onset time of ICMEs observed at large distances from the Sun. We have developed a data cube containing several thousand modeled elongation-time plots for CMEs traveling with various speeds and directions. Each curve represents an elongation-time plot for combinations of the following parameters: Speed V = [0, 100, 200, ..., 4000] km/s; latitude Λ = [0, 15, 30, ..., and 90]°; longitude Φ = [1, 5, 15, 30, 45, ..., and 90]°. We passed this cube across the elongation-time data for each of the 207 SMEI ICMEs, moving at increments of 30 min, and assigned the curve of best fit to the data. This was achieved by summing the differences between each point in the SMEI data and the modeled curve and selecting the curve that produced the smallest difference sum. This was confirmed by choosing the average of the model-data differences and selecting the smallest average. In both cases the same curve was identified for each event.

[13] Once the best modeled elongation-time fit has been identified, we can examine the parameters required to produce the curve. Hence for every SMEI ICME event we have not only the onset time of the ICME and the appearance of its elongation evolution as a function of time, but also the speed and direction (latitude, longitude) of the measured point on the ICME front. The procedure described above is henceforth referred to as the Cube-Fit procedure. (This is not to be confused with ''cubic fit'', which is the determination of a least squares third-order polynomial to the data, an operation not performed in the present study.)

[14] By also assigning a linear fit to the SMEI data we now have two onset times for each event. The first, based on the Cube-Fit plot and the second from the linear fit. We then examined LASCO data in the same quadrant of the sky as the SMEI event, starting 24 h before the earliest onset time and 12 h after the latest onset time, except in the cases

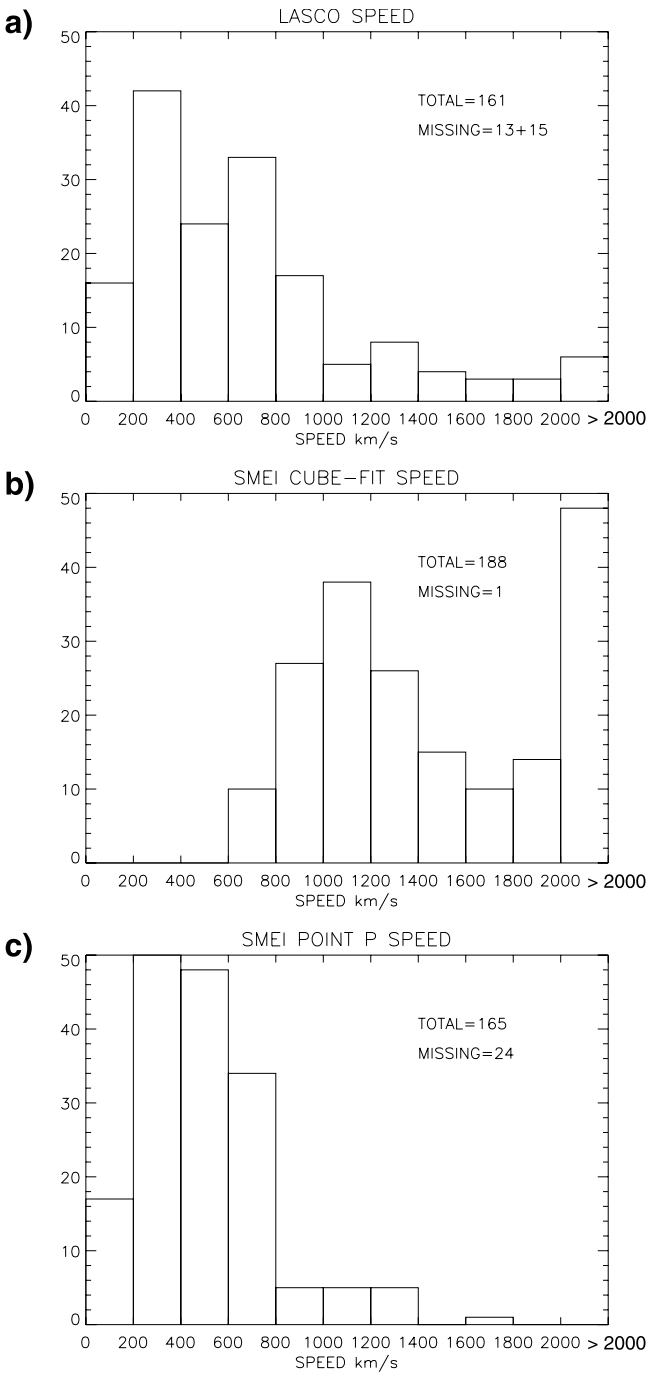

Figure 2. Histograms of (a) projected LASCO speed for the associated LASCO CMEs, (b) Cube-Fit speed for the SMEI ICMEs, and (c) Point P approximation speeds for the 189 SMEI events for which there was full LASCO coverage. In all three panels event numbers are shown in blocks of 200 km/s intervals.

where the first data point of the SMEI ICME appears during those 12 h. Here we define ''quadrant'' as the region of the sky centered on the SMEI transient and spanning 45° position angle (PA) on either side. For example, for the SMEI event that first appeared on 6 August 2003, the Cube-Fit onset time is ~12:00 UT on 3 August and the linear onset time is ~20:00 UT on 4 August. Hence we examine the LASCO data during 3–6 August around the northwestern quadrant of the sky, that corresponds to the quadrant in which the SMEI ICME was detected. For this event there is a LASCO CME that matches well with the data, first appearing at 21:30 UT on 3 August. Henceforth, all times are referred to in UT. Figure 3 shows the elongation-time plot of the event from both the LASCO and SMEI data, along with several other events. The two SMEI events on 4 and 6–7 August were each found to be clearly associated with a LASCO CME, and their respective plots are shown. In each case the LASCO data matches more accurately with the Cube-Fit (dashed curve) than the linear fit (solid straight line). We believe that the events observed in LASCO and SMEI in both cases are the same phenomena and thus, these are examples of clear associations between LASCO and SMEI. Other examples of SMEI ICMEs that have been associated with LASCO CMEs are given by *Tappin et al.* [2004] and *Howard et al.* [2006, 2007].

[15] We should also note that the reference frames for SMEI and LASCO are slightly different, due to the coordinate system chosen in the processing of the data from both instruments. For LASCO, the heliographic coordinate system is chosen, while SMEI is analyzed in ecliptic coordinates. The difference between the two systems varies as the year progresses but the maximum difference between the two is 7.25° on 3 June and 3 December for a nonleap year. Given that we are considering entire quadrants we have disregarded this difference.

3.2. Cube-Fit and LASCO Speeds

[16] The Cube-Fit was used as an alternative limit to the linear fit through the elongation-time plot. The parameters assigned to the Cube-Fit curve (direction, speed) were simply for the curve that best matched the SMEI data (i.e., the curve with the smallest collective distance from the SMEI data points). This does not mean there may be other curves (e.g., with lower speeds and different directions) that could meet the data almost as well. It is possible with further analysis of each event we may produce curves that seem more physical. However, we wanted to create a procedure as automated as possible in order to remove bias. The advantages of this have already been discussed and the disadvantages are discussed later in this paper.

[17] While we may regard the Cube-Fit procedure as more accurate, it is not without its limitations. The assumption is of a single point moving with a fixed speed and trajectory through the heliosphere, and the procedure does not attempt to account for the possibility that different parts of the ICME may be measured at different times. This is most likely to occur at higher elongation angles. The constant speed assumption is also oversimplified, but the computing time required for adding another dimension (i.e., acceleration) to the data cube was prohibitive.

[18] In order to evaluate the validity of the Cube-Fit model refer to Figure 2. Here are histograms of projected LASCO speed and Cube-Fit speed for the SMEI ICMEs for the 189 SMEI events for which there was full LASCO coverage. Also shown is the histogram for the Point P speeds, determined using the Point P approximation to convert elongation to distance [*Howard*, 2006; *Webb et al.*, 2006]. The Point P speeds appear to match the projected

Table 1. List of the 207 Events Detected by SMEI and Their LASCO Counterpart During the Time Period of the Present Study[a]

No.	SMEI Date Time PA	SMEI Speed Direction	Onset Time Point P Speed	LASCO Time PA Width Speed	Comments	?
001	2003/02/08 ~5UT 044	800 km/s N75E75	2003/02/07 04:24 232	2003/02/06 04:30:05 067 114 322 2003/02/07 08:42:05 035 020 301	Second CME is narrow and not listed in CDAW.	W
002	2003/02/10 ~8UT 232	600 km/s S00W45	2003/02/10 20:41 339	No LASCO association		N
003	2003/02/12 ~0UT 031	1200 km/s N30E60	2003/02/11 23:52 –	2003/02/11 18:54:05 245 100 285		Y
004	2003/02/13 ~3UT 106	1400 km/s S75E75	2003/02/12 21:27 494	2003/02/12 06:30:05 101 066 200 2003/02/13 02:30:05 098 027 409		Y
005	2003/02/14 ~8UT 096	600 km/s S30E60	2003/02/14 08:04 283	2003/02/14 08:06:05 284 097 174 2003/02/14 20:06:05 266 065 796	Could be a merger of the two CMEs.	Y
006	2003/02/14 ~20UT 280	600 km/s N30W60	2003/02/14 22:53 288	2003/02/15 08:06:05 256 163 577 2003/02/15 14:06:05 276 060 552	Later CME may catch up with earlier.	Y
007	2003/02/18 ~9UT 331	1200 km/s N45W30	2003/02/18 13:16 602	2003/02/18 02:42:06 312 093 888	*Howard et al.* [2007]	Y
008	2003/02/19 ~3UT 359	800 km/s N15W45	2003/02/19 14:59 394	2003/02/19 12:08:05 310 064 075	Very slow in LASCO's FOV	W
009	2003/02/18 ~23UT 019	600 km/s N30E05	2003/02/20 08:05 414	2003/02/20 12:08:06 024 072 124		Y
010	2003/02/21 ~12UT 157	800 km/s S60E45	2003/02/21 12:31 379	2003/02/20 06:30:05 148 061 166 2003/02/20 11:30:05 193 254 1026	Both CMEs possible.	Y
011	2003/02/22 ~20UT 141	800 km/s S45E75	2003/02/22 09:40 314	2003/02/22 01:31:42 158 093 158		Y
012	2003/02/23 ~7UT 145	800 km/s S45E60	2003/02/23 06:57 348	2003/02/23 12:18:42 055 012		W
013	2003/02/27 ~20UT 328	800 km/s N60W75	2003/02/27 00:43 254	missing LASCO Data	2003/02/24 15:00–2003/02/27 17:00	O
014	2003/02/28 ~0UT 131	800 km/s S00E45	2003/02/28 13:05 450	missing LASCO Data	2003/02/24 15:00–2003/02/27 17:00	O
—	2003/03/01 ~7UT 125	800 km/s S60E45	2003/03/01 07:04 450	2003/03/01 13:54:24 078 048 357	same ICME as previous	Y
015	2003/02/28 ~20UT 109	600 km/s S60E75	2003/02/28 02:32 200	2003/02/28 18:30:05 138 041 648 2003/02/28 23:25 ADD	second CME is faint and not listed in CDAW	Y
016	2003/03/01 ~7UT 176	600 km/s S15E60	2003/03/01 15:30 354	2003/03/01 15:54:05 077 047 420		Y
017	2003/03/03 ~12UT 083	1600 km/s N00E90	2003/03/03 10:24 462	2003/03/03 04:06:05 077 040 361		Y
—	2003/03/03 ~12UT 085	1200 km/s N45E05	2003/03/03 19:32 682	2003/03/03 21:08:06 114 201 702	Same CME as previous.	Y
—	2003/03/03 ~19UT 082	1400 km/s N00E90	2003/03/02 10:53 682	2003/03/03 21:08:06 114 201 702	Same CME as previous.	Y
018	2003/03/05 ~17UT 335	800 km/s N60W75	2003/03/05 09:44 300	2003/03/04 20:20 ADD 2003/03/05 02:18:05 352 070 240	Very faint CME. Missed by CDAW.	W
019	2003/03/10 ~23UT 044	800 km/s N45E60	2003/03/10 22:34 374	2003/03/10 06:30:05 048 037 271 2003/03/10 10:54:31 37 66 337 2003/03/10 16:54:05 30 59 330	merger?	Y
020	2003/03/13 ~6UT 054	2000 km/s N30E75	2003/03/13 04:08 397	2003/03/13 02:54:05 056 091 1020		Y
021	2003/03/12 ~10UT 020	1000 km/s N00E90	2003/03/12 06:08 855	2003/03/12 03:30:05 007 050 477 2003/03/12 23:06:05 060 037 478	Likely CME not listed in CDAW.	W
022	2003/03/16 ~0UT 008	800 km/s N45E05	2003/03/16 11:33 494	2003/03/15 21:54:23 063 125 596		Y
023	2003/03/18 ~16UT 336	1000 km/s N75W45	2003/03/18 15:27 425	2003/03/18 13:54:05 Halo 360 1042 2003/03/19 02:30:05 Halo 360 1342	merger?	Y
024	2003/03/21 ~11UT 349	800 km/s N00W60	2003/03/21 16:28 430	2003/03/20 10:54:06 054 066 481		Y
—	2003/03/21 ~17UT 350	1000 km/s N45W30	2003/03/22 00:06 526	2003/03/20 19:40:05 342 050 072	Same ICME as previous.	W
025	2003/03/21 ~15UT 001	800 km/s N15E15	2003/03/23 05:23 610	2003/03/22 02:30:05 330 060 028	CME very faint not listed in CDAW.	W
026	2003/03/25 ~10UT 342	1000 km/s N60W75	2003/03/25 08:17 428	2003/03/25 12:30:05 282 012 686 2003/03/25 12:54:05 357 067 580		Y
027	2003/03/23 ~11UT 342	1000 km/s N60W75	2003/03/26 10:48 432	2003/03/25 19:31:40 000 065 343		Y
028	2003/04/05 ~2UT 311	1000 km/s N00W90	2003/04/04 22:08 362	2003/04/04 09:30:05 292 031 424 2003/04/04 18:50:05 300 041 216	*Howard et al.* [2006]	Y
—	2003/04/05 ~2UT 293	800 km/s N60W45	2003/04/05 374	2003/04/04 21:19:51 291 089 487	Same ICME as previous.	Y
029	2003/04/06 ~0UT 072	3000 km/s N60E05	2003/04/04 04:27 100	2003/04/04 08:54:31 073 023 342	*Tappin* [2006]	Y
030	2003/04/16 ~2UT 015	2000 km/s N60E60	2003/04/14 02:48 197	No LASCO association.		N
031	2003/04/18 ~6UT 009	1200 km/s N15E30	2003/04/18 23:09 128	2003/04/18 15:26 45 45	Very slow narrow streamer blowout.	W
032	2003/04/18 ~12UT 017	2000 km/s N60E05	2003/04/16 16:51 299	2003/04/18 15:26 45 45	Very slow narrow streamer blowout.	W

Table 1. (continued)

No.	SMEI Date Time PA	SMEI Speed Direction	Onset Time Point P Speed	LASCO Time PA Width Speed	Comments	?
033	2003/04/23 ~12UT 330	1000 km/s N15W30	2003/04/24 07:05 621	2003/04/23 01:27:14 271 248 916 2003/04/23 16:50:05 343 105 596	*Howard et al.* [2006]	Y
034	2003/04/24 ~12UT 312	800 km/s N75W05	2003/04/24 12:13 337	2003/04/24 13:27:14 317 242 609		Y
035	2003/04/27 ~3UT 290	1000 km/s N45W75	2003/04/27 04:51 481	2003/04/27 00:06:07 288 035 386 2003/04/27 01:27:17 273 094 438 2003/04/27 04:26:05 300 087 746		Y
036	2003/04/27 ~15UT 038	2200 km/s N75E45	2003/04/26 19:40 391	2003/04/26 21:50:05 048 166 672 2003/04/27 03:26:12 050 082 547		Y
037	2003/04/30 ~15UT 358	1200 km/s N30W60	2003/04/29 11:13 194	2003/04/30 00:26:05 308 024 369 2003/04/30 13:50:05 039 043 399		Y
038	2003/05/03 ~16UT 025	1600 km/s N60E45	2003/05/02 23:20 291	2003/05/02 23:50:05 007 143 359		Y
039	2003/05/04 ~3UT 026	2200 km/s N00E90	2003/05/02 19:29 334	2003/05/03 10:50:05 019 045 247	CME not listed in CDAW	W
040	2003/05/04 ~17UT 343	3800 km/s N75W75	2003/05/03 17:21 11:53 434	2003/05/04 16:06:05 338 030 275	Faint narrow CME. Not listed.	W
041	2003/05/12 ~18UT 017	2000 km/s N75E75	2003/05/11 11:53 301	2003/05/11 20:58:42 328 194 714		Y
042	2003/05/20 ~0UT 004	3400 km/s N60E90	2003/05/19 04:47 504	2003/05/19 09:50:05 023 101 866		Y
043	2003/05/28 ~3UT 285	2800 km/s N15W60	2003/05/28 00:23 758	2003/05/27 23:50:05 Halo 360 964	*Howard et al.* [2006]	Y
—	2003/05/27 ~17UT 002	1600 km/s N15E15	2003/05/28 18:25 758	2003/05/28 00:50:05 Halo 360 1366	Same ICME as previous.	Y
044	2003/05/28 ~12UT 237	1000 km/s S00W60	2003/05/28 08:11 324	2003/05/28 00:50:05 Halo 360 1366 2003/05/29 01:27:12 Halo 360 1237	*Tappin et al.* [2004] and *Howard et al.* [2006]	Y
045	2003/05/30 ~17UT 248	1800 km/s S15W30	2003/05/31 02:47 1164	2003/05/30 11:06:06 198 058 245 2003/05/31 02:30:19 Halo 360 1835		Y
046	2003/06/01 ~20UT 239	2200 km/s S15W75	2003/06/01 18:26 778	2003/06/02 00:30:07 265 172 1656		Y
047	2003/06/01 ~17UT 014	1200 km/s N15E60	2003/06/01 16:36 432	2003/06/01 01:54:42 069 063 350 2003/06/01 03:30:23 087 083 1270		Y
—	2003/06/01 ~19UT 351	1000 km/s N75W30	2003/05/31 00:59 216	2003/06/02 08:54:05 261 161 980	Same ICME as previous.	Y
048	2003/06/05 ~20UT 009	800 km/s N15E45	2003/06/06 04:57 324	2003/06/06 14:54:05 019 037 243		Y
049	2003/06/12 ~10UT 305	2200 km/s N75W75	2003/06/12 04:53 715	missing LASCO data	2003/06/10 15:00–2003/06/13 15:00	O
050	2003/06/11 ~17UT 326	800 km/s N15W30	2003/06/12 18:54 489	missing LASCO data	2003/06/10 15:00–2003/06/13 15:00	O
051	2003/06/12 ~17UT 320	1000 km/s N15W30	2003/06/13 12:39 562	2003/06/13 16:30:57 288 067 346		Y
052	2003/06/23 ~10UT 261	1400 km/s S45E05	2003/06/23 16:37 804	2003/06/23 12:30:05 257 046 663		Y
053	2003/06/22 ~18UT 032	1000 km/s N75E05	2003/06/22 03:20 306	2003/06/20 06:54:05 023 033 2003/06/20 20:06:05 053 055		Y
054	2003/06/24 ~10UT 332	1000 km/s N15W30	2003/06/25 08:36 456	missing LASCO data	2003/06/23 18:00–2003/07/02 18:00	O
055	2003/07/02 ~0UT 346	1000 km/s N30W60	2003/06/30 22:11 182	missing LASCO data	2003/06/23 18:00–2003/07/02 18:00	O
056	2003/07/08 ~3UT 357	1400 km/s N00W60	2003/07/08 10:44 411	partial LASCO data	2003/07/02 15:00–2003/07/10 16:00	O
057	2003/07/08 ~16UT 309	800 km/s N30W45	2003/07/08 08:53 372	partial LASCO data	2003/07/02 15:00–2003/07/10 16:00	O
058	2003/07/10 ~3UT 332	800 km/s N15W30	2003/07/11 02:34 518	partial LASCO data	2003/07/02 15:00–2003/07/10 16:00	O
—	2003/07/11 ~3UT 243	1000 km/s S75W75	2003/07/10 21:49 378	Same ICME as previous.		O
059	2003/07/17 ~21UT 351	1200 km/s N45W05	2003/07/18 05:54 520	2003/07/17 08:54:05 141>298 531		Y
060	2003/07/20 ~21UT 323	1000 km/s N15W15	2003/07/22 04:33 792	2003/07/20 05:30:17 334 100 320 2003/07/22 02:54:06 318 044 210	CMEs are too slow but the onset times match.	W
061	2003/07/20 ~4UT 360	800 km/s N30E05	2003/07/22 14:52 336	2003/07/20 10:30:05 343 053 294	Faint CME.	W
062	2003/07/22 ~15UT 298	800 km/s N30W05	2003/07/23 12:01 505	2003/07/23 12:30:05 213 123 329		Y
063	2003/07/23 ~17UT 307	800 km/s N15W30	2003/07/24 14:32 437	2003/07/24 03:06:05 282 039 195		Y
064	2003/07/24 ~18UT 309	1200 km/s N45W01	2003/07/24 21:55 336	No LASCO association.		N
065	2003/07/23 ~10UT 088	1400 km/s N15E05	2003/07/23 16:59 1222	No LASCO association.		N
066	2003/07/24 ~0UT 006	1400 km/s N15E01	2003/07/25 11:32 1222	2003/07/24 21:30:10 039 050 265		Y
067	2003/07/25 ~16UT 290	3000 km/s N15W15	2003/07/26 03:32 123	2003/07/25 18:30:06 286 020 302	Tiny faint CME.	W
—	2003/07/26 ~9UT 231	4000 km/s N15W15	2003/07/26 03:20 123	2003/07/25 18:30:06 286 020 302	Same ICME as previous.	W

Table 1. (continued)

No.	SMEI Date Time PA	SMEI Speed Direction	Onset Time Point P Speed	LASCO Time PA Width Speed	Comments	?
068	2003/07/27 ~8UT 350	1000 km/s N15W30	2003/07/28 08:30 567	2003/07/28 02:30:00 350 020 106	Very faint narrow CME. Not listed.	W
069	2003/07/30 ~18UT 331	1000 km/s N30W60	2003/07/29 23:01 237	2003/07/28 21:34:05 350 030 142	Faint narrow CME. Not listed.	W
070	2003/07/31 ~21UT 352	600 km/s N30W30	2003/08/01 18:19 256	2003/08/01 00:54:05 322 037 179		Y
071	2003/08/03 ~12UT 330	800 km/s N30W05	2003/08/04 20:08 452	2003/08/03 21:30:08 270 112 290		Y
072	2003/08/12 ~13UT 052	600 km/s N00E30	2003/08/14 11:23 331	2003/08/13 06:54:06 067 022 445	Halo CME is too slow to be ICME.	W
				2003/08/14 20:06:05 Halo 360 378	Other CME faint and narrow.	
073	2003/08/20 ~0UT 269	2600 km/s S00W90	2003/08/19 14:26 632	2003/08/18 14:30:05 281 058		Y
				2003/08/18 20:54:28 282 65		
				2003/08/19 04:30:29 259 64		
				2003/08/19 05:30:07 288 57		
				2003/08/19 08:30:31 257 35		
				2003/08/19 09:30:05 258 112		
				2003/08/19 10:30:23 262 111		
074	2003/08/19 ~18UT 295	800 km/s N30W45	2003/08/20 01:33 433	2003/08/19 05:30:07 288 057 324		Y
				2003/08/19 09:30:05 258 112 300		
				2003/08/19 10:30:23 262 111 468		
075	2003/08/27 ~14UT 340	2600 km/s N60W75	2003/08/26 00:08 271	2003/08/26 23:26:05 355 037 162	Neither CME listed.	W
				2003/08/27 10:50:05 345 044 140		
076	2003/09/01 ~2UT 269	1200 km/s S75W60	2003/08/31 22:31 465	2003/08/31 06:30:05 248 111 353		Y
077	2003/09/07 ~18UT 252	1400 km/s S00W75	2003/09/07 17:57 655	2003/09/07 14:30:05 227 072 376		Y
				2003/09/07 16:54:05 245 116 685		
078	2003/09/15 ~12UT 268	600 km/s S60W60	2003/09/15 19:22 313	2003/09/16 00:54:05 264 049 268		Y
079	2003/09/19 ~23UT 276	1000 km/s N00W45	2003/09/20 04:37 518	2003/09/20 04:30:05 258 145 653		Y
				2003/09/20 09:30:12 280 105 853		
080	2003/10/10 ~22UT 101	3400 km/s S45E05	2003/10/09 04:52 –	2003/10/09 03:06:05 037 115 529		Y
081	2003/10/18 ~3UT 108	800 km/s S45E05	2003/10/18 13:37 430	2003/10/17 16:06:05 143 134 189		Y
				2003/10/18 15:30:20 Halo 360 627		
082	2003/10/22 ~21UT 328	1000 km/s N30W05	2003/10/22 15:23 668	2003/10/22 20:06:05 093 134 1085	*Howard et al.* [2006]	Y
—	2003/10/21 ~21UT 190	1800 km/s S30E75	2003/10/22 18:36 704	2003/10/22 03:54:05 104 101 1163	Same ICME as previous.	Y
083	2003/10/22 ~20UT 326	1600 km/s N15W75	2003/10/22 19:55 537	2003/10/22 20:06:05 093 134 1085	*Howard et al.* [2006]	Y
084	2003/10/22 ~21UT 332	1600 km/s N30W75	2003/10/22 11:51 483	2003/10/22 08:30:32 286>267 719	*Howard et al.* [2006]	Y
—	2003/10/23 ~15UT 294	3400 km/s N15W15	2003/10/23 19:50 51	2003/10/23 20:06:05 103 095 1136	Same ICME as previous.	Y
085	2003/10/22 ~21UT 101	2000 km/s S15E15	2003/10/23 09:22 –	2003/10/23 03:06:05 102 046 656	*Howard et al.* [2006]	Y
086	2003/10/26 ~0UT 276	1200 km/s N30W30	2003/10/26 09:34 703	2003/10/26 01:31:46 256 075 419	*Howard et al.* [2006] and *Jackson et al.* [2006]	Y
				2003/10/26 05:30:05 267 086 684		
				2003/10/26 17:54:05 270 171 1537		
087	2003/10/27 ~0UT 115	1200 km/s S00E15	2003/10/28 09:52 1611	2003/10/27 20:30:06 312 043 990	*Howard et al.* [2006] and *Jackson et al.* [2006]	Y
				2003/10/28 06:30:05 299 015 684		
				2003/10/28 11:30:05 Halo 360 2459		
088	2003/10/28 ~12UT 297	4000 km/s N15W75	2003/10/28 11:48 1054	2003/10/28 07:31:43 114 016 394	*Howard et al.* [2006] and *Jackson et al.* [2006]	Y
				2003/10/28 10:54:05 124 147 1054		
				2003/10/28 11:30:05 Halo 360 2459		
089	2003/10/30 ~4UT 324	2400 km/s N30W60	2003/10/30 04:06 856	2003/10/29 20:54:05 Halo 360 2029		Y
090	2003/11/01 ~20UT 299	1000 km/s N30W45	2003/11/02 03:20 1322	2003/11/01 14:54:05 274 055 334	*Howard et al.* [2006]	Y
				2003/11/01 23:06:53 254 093 899		
				2003/11/02 09:30:05 Halo 360 2036		
091	2003/11/01 ~22UT 270	1800 km/s N15W05	2003/11/02 14:33 1322	2003/11/02 09:30:05 Halo 360 2036	*Howard et al.* [2006]	Y

Table 1. (continued)

No.	SMEI Date Time PA	SMEI Speed Direction	Onset Time Point P Speed	LASCO Time PA Width Speed	Comments	?
				2003/11/02 17:30:05 Halo 360 2598		
092	—	—	— 540	2003/11/01 20:40:00 310 325 —	Determined from SMEI timing.	Y
093	2003/11/05 ~22UT 142	2800 km/s S30E05	2003/11/06 05:33 279	2003/11/06 17:30:05 Halo 360 1523		Y
094	2003/11/06 ~9UT 089	4000 km/s N30E01	2003/11/05 02:28 172	2003/11/04 19:54:05 Halo 360 2657	halo CME too early other CMEs faint	W
095	2003/11/13 ~12UT 129	1600 km/s S00E60	2003/11/13 15:16 836	2003/11/13 05:30:05 103 062 598	*Howard et al.* [2006]	Y
096	2003/11/18 ~11UT 150	3400 km/s S30E45	2003/11/18 09:08 775	2003/11/18 08:06:05 144 104 1223	*Howard et al.*, [2006]	Y
				2003/11/18 08:50:05 Halo 360 1660		
097	2003/11/17 ~21UT 127	1200 km/s S30E45	2003/11/18 01:59 775	2003/11/18 08:06:05 144 104 1223	*Howard et al.* [2006]	Y
				2003/11/18 08:50:05 Halo 360 1660		
098	2003/11/19 ~17UT 111	2600 km/s S00E05	2003/11/20 19:16 615	2003/11/20 08:06:05 Halo 360 669		Y
099	2003/11/20 ~0UT 324	1400 km/s N30W60	2003/11/19 23:19 615	2003/11/19 09:26:05 307 084 422		Y
				2003/11/20 08:06:05 Halo 360 669		
				2003/11/20 08:06:05 242 047 890		
100	2003/11/28 ~21UT 135	1200 km/s S75E75	2003/11/28 15:47 433	2003/11/28 10:06:05 146 093 248		Y
101	2003/12/31 ~4UT 141	2600 km/s S60E90	2003/12/29 21:00 324	2003/12/29 08:25:05 125 061		Y
102	2004/01/02 ~0UT 092	1200 km/s N30E30	2004/01/02 10:55 714	2004/01/02 13:00:05 111 054 757		Y
				2004/01/02 16:20:05 105 074 924		
103	2004/01/05 ~2UT 118	2000 km/s S15E45	2004/01/05 08:10 1094	2004/01/05 09:40:05 124 046 795	*Howard et al.* [2006]	Y
				2005/01/05 18:00:06 105 80 550		
				2005/01/05 21:17:49 122 51 1207		
104	2004/01/08 ~2UT 122	1000 km/s S00E15	2004/01/10 03:41 188	2004/01/08 05:06:05 083 144 1713	steady stream of events	Y
				2004/01/08 14:54:05 097 127 147	Throughout the day.	
				2004/01/09 02:06:05 135 051 1217	merger?	
105	2004/01/13 ~2UT 116	1000 km/s S30E60	2004/01/13 04:38 508	2004/01/12 15:30:05 109 082 244	Merger of the two events?	Y
				2004/01/13 06:54:05 105 024 657	Some other LASCO events nearby.	
106	2003/01/19 ~2UT 134	1000 km/s S30E60	2004/01/19 01:19 400	2004/01/20 00:06:05 Halo 360 965	Halo CME too late to match SMEI data.	W
107	2004/01/20 ~23UT 119	4000 km/s S60E45	2004/01/19 05:38 180	2004/01/20 08:30:05 186 096 590	High elongation angles.	Y
108	2004/01/21 ~12UT 117	2400 km/s S75E75	2004/01/21 09:24 793	2004/01/20 04:54:05 Halo 360 762	*Howard et al.* [2006]	Y
109	2004/01/20 ~20UT 133	800 km/s S30E05	2004/01/21 17:30 509	2004/01/20 12:30:05 129 111 727		Y
110	2004/01/23 ~11UT 145	800 km/s S45E15	2004/01/23 22:30 459	2004/01/23 13:32:16 108 086 254		Y
111	2004/02/06 ~12UT 033	1200 km/s N30E45	2004/02/03 23:31 379	2004/02/03 02:54:05 046 047 340		W
				2004/02/03 09:06:05 50 59 364		
				2004/02/06 04:06:05 36 22 589		
—	2004/02/05 ~21UT 058	2400 km/s N60E90	2004/02/05 11:33 379	2004/02/06 04:06:05 036 022 589	Same ICME as previous.	W
112	2004/02/08 ~17UT 018	1200 km/s N30E30	2004/02/08 01:42 –	2004/02/07 08:30:05 015 023 450	narrow faint CME	W
—	2004/02/07 ~22UT 020	2600 km/s N60E90	2004/02/07 14:41 –	2004/02/07 08:30:05 015 023 450	Same ICME as previous.	W
—	2004/02/08 ~14UT 016	1200 km/s N30E05	2004/02/08 18:45 –	No LASCO association.	Same ICME as previous.	W
—	2004/02/10 ~8UT 033	3200 km/s N45E15	2004/02/08 22:12 –	No LASCO association.	Same ICME as previous.	W
113	2004/02/14 ~17UT 115	800 km/s S15E60	2004/02/14 19:56 401	2004/02/15 03:54:05 107 126 637	*Howard et al.* [2007]	Y
114	2004/02/20 ~13UT 198	1600 km/s S30E75	2004/02/20 13:33 717	LASCO outflow cannot measure	Nothing to measure a speed from.	W
115	2004/03/07 ~10UT 358	1000 km/s N30W30	2004/03/07 23:00 377	2004/03/07 06:06:05 287 83 534	Could be the outer flanks	Y
				2004/03/07 07:31:39 239 043 620	of these CMEs.	
116	2004/03/09 ~18UT 341	1200 km/s N75W75	2004/03/09 13:57 457	2004/03/09 22:30:00 320 014 45	narrow, faint CME	W
117	2004/03/25 ~7UT 004	1000 km/s N75E45	2004/03/25 01:31 370	Partial LASCO Data	2004/03/19–2004/04/04	O
118	2004/03/27 ~21UT 327	1000 km/s N15W75	2004/03/27 20:34 427	Partial LASCO Data	2004/03/19–2004/04/04	O
119	2004/03/30 ~4UT 002	1200 km/s N60E75	2004/03/29 23:32 447	Partial LASCO Data	2004/03/19–2004/04/04	O
120	2004/03/31 ~20UT 020	1000 km/s N15E05	2004/04/02 21:20 391	Partial LASCO Data	2004/03/19–2004/04/04	O
121	2004/04/02 ~15UT 357	1000 km/s N15W60	2004/04/02 16:03 413	2004/04/01 22:00:05 059 079 460	partial LASCO data	Y
122	2004/04/02 ~0UT 044	1200 km/s N15E30	2004/04/02 08:26 142	2004/04/02 11:00:05 056 034 84	partial LASCO data	Y
123	2004/04/12 ~21UT 026	3600 km/s N75E30	2004/04/11 18:53 355	2004/04/11 11:54:05 Halo 360 1132		Y

Table 1. (continued)

No.	SMEI Date Time PA	SMEI Speed Direction	Onset Time Point P Speed	LASCO Time PA Width Speed	Comments	?
				2004/04/12 11:06:05 033 050 453		
124	2004/02/23 ~18UT 275	1000 km/s N75W45	2004/04/22 16:25 234	Missing LASCO Data	2004/04/20 05:37–2004/04/29 12:00	O
125	2004/04/29 ~6UT 015	1400 km/s N00E60	2004/04/28 22:01 343	2004/04/29 19:27:14 Halo 360 185		Y
126	2004/05/06 ~22UT 023	800 km/s N15E45	2004/05/07 01:36 241	2004/05/07 10:50:05 097 094 469	All events very faint near N pole.	Y
				2004/05/07 14:50:05 196 118 388	Could be a flank of one CME.	
				2004/05/07 14:50:05 304 150 169		
				2004/05/07 19:27:08 047 088 169		
127	2004/05/21 ~22UT 357	2800 km/s N75W75	2004/05/21 00:48 425	2004/05/20 00:50:05 308 053 427	Faint narrow CME.	W
128	2004/05/22 ~20UT 354	3000 km/s N60W75	2004/05/21 18:04 380	2004/05/22 04:26:05 327 020 340	Very faint narrow CME.	W
129	2005/05/27 ~8UT 013	3800 km/s N75E75	2004/05/25 18:00 295	No LASCO association.		N
130	2004/05/26 ~8UT 008	800 km/s N15E30	2004/05/27 12:45 431	No LASCO association.		N
131	2004/06/22 ~15UT 306	1600 km/s N45W75	2004/06/22 12:11 625	missing LASCO data	2004/06/20 13:30–2004/06/24 14:00	O
132	2004/06/27 ~12UT 290	800 km/s N30W30	2004/06/28 02:15 488	missing LASCO Data	2004/06/28 02:12–13:36,17:12–23:36	O
133	2004/07/08 ~18UT 297	1000 km/s N15W30	2004/07/09 13:40 576	2004/07/09 06:30:05 268 050 577	Same CME as following?	Y
134	2004/07/08 ~18UT 303	1000 km/s N15W30	2004/07/09 12:33 576	2004/07/09 06:30:05 268 050 577	Same CME as previous?	Y
135	2004/07/13 ~2UT 333	800 km/s N45W05	2004/07/13 17:13 350	2004/07/13 00:54:05 313 088 607	*Howard et al.* [2006]	Y
				2004/07/13 00:54:05 253 201 409		
				2004/07/13 09:30:05 Halo 360 747		
136	2004/07/19 ~19UT 278	1400 km/s N00W90	2004/07/19 11:43 464	2004/07/19 09:30:05 286 090 790	*Howard et al.* [2006]	Y
137	2004/07/19 ~22UT 348	1200 km/s N00W30	2004/07/20 19:26 728	2004/07/20 13:31:52 Halo 360 710	Same CME as following?	Y
138	2004/07/20 ~2UT 302	1200 km/s N30W30	2004/07/20 14:37 715	2004/07/20 13:31:52 Halo 360 710	Same CME as following?	Y
139	2004/07/28 ~3UT 243	1200 km/s S15W75	2004/07/27 22:04 483	2004/07/27 06:06:05 207 082 436	Could be a merger.	Y
				2004/07/27 14:06:05 236 041 381		
				2004/07/27 15:54:05 228 074 406		
				2004/07/28 03:30:05 220>201 754		
140	2004/08/13 ~22UT 266	1000 km/s S30W30	2004/08/14 07:54 571	2004/08/14 02:30:05 263 091 307		Y
141	2004/08/15 ~14UT 313	1000 km/s N60W05	2004/08/15 08:31 299	2004/08/14 21:54:05 222 143 252		Y
142	2004/09/01 ~4UT 266	1000 km/s S00W90	2004/08/31 22:56 380	2004/08/31 05:54:05 272 070 311	Same CME as following.	Y
				2004/08/31 07:54:05 268 053 132		
				2004/08/31 14:54:05 265 076 503		
				2004/09/01 03:30:05 260 067 401		
—	2004/09/01 ~6UT 266	1000 km/s S00W75	2004/09/01 04:24 443	2004/09/01 03:30:05 260 067 401	Same CME as previous.	Y
				2004/09/01 15:38:12 Halo 360 420		
143	2004/09/12 ~16UT 092	3600 km/s S00E30	2004/09/12 15:52 –	Same CME as following.		Y
				2004/09/12 00:36:06 Halo 360 1328		
—	2004/09/11 ~3UT 090	1400 km/s N15E05	2004/09/12 13:57 –	Same CME as previous.		Y
				2004/09/12 00:36:06 Halo 360 1328		
144	2004/09/15 ~12UT 123	3400 km/s S00E90	2004/09/15 00:40 663	No LASCO association.		N(Y)
—	2004/09/14 ~2UT 120	1000 km/s S15E45	2004/09/14 14:34 518	2004/09/14 03:12:09 135 106 271	Same ICME as previous.	Y
				2004/09/14 10:12:05 Halo 360 462		
145	2004/09/20 ~2UT 269	2200 km/s S00W90	2004/09/19 22:55 744	2004/09/19 22:18:13 262 099		Y
—	2004/09/18 ~13UT 271	800 km/s N30W05	2004/09/19 10:27 505	Same ICME as previous.		O
146	2004/10/11 ~10UT 333	1600 km/s N60W05	2004/10/10 03:56 188	2004/10/10 11:00:32 298 043 303	Faint CME.	W
147	2004/10/29 ~2UT 294	600 km/s N30W30	2004/10/29 19:57 316	2004/10/29 05:06:05 302 043 454		Y
				2004/10/30 03:54:09 320 060 138		
				2004/10/30 06:54:05 Halo 360 422		
				2004/10/30 09:54:05 265 074 552		
				2004/10/30 12:30:06 Halo 360 427		
				2004/10/30 16:54:05 Halo 360 690		
148	2004/11/02 ~12UT 054	1000 km/s N75E30	2004/11/01 20:13 288	2004/11/01 03:54:05 242>192 459		Y

Table 1. (continued)

No.	SMEI Date Time PA	SMEI Speed Direction	Onset Time Point P Speed	LASCO Time PA Width Speed	Comments	?
				2004/11/01 06:06:05 266 146		
149	2004/11/02 ~2UT 093	1000 km/s S00E30	2004/11/02 15:25 –	2004/11/03 03:54:05 091>239 918		Y
150	2004/11/03 ~17UT 123	1000 km/s S00E15	2004/11/05 20:50 –	2004/11/03 16:06:05 Halo 360 1068		Y
				2004/11/03 18:54:05 045 107 513		
				2004/11/04 09:54:05 Halo 360 653		
				2004/11/04 23:30:05 338>293 1055		
				2004/11/06 01:31:51 Halo 360 818		
151	2004/11/07 ~18UT 313	2800 km/s N15W45	2004/11/07 08:47 252	2004/11/07 03:18:05 322 048 316		Y
				2004/11/07 06:30:05 330 055 300		
				2004/11/07 09:54:06 325 030 467		
—	2004/11/08 ~3UT 328	3200 km/s N75W05	2004/11/07 20:04 861	2004/11/07 14:30:05 286 100 226	Same ICME as previous.	Y
				2004/11/07 16:54:05 Halo 360 1759		
				2004/11/07 22:30:05 324 020 424		
152	2004/11/30 ~14UT 349	1000 km/s N00W30	2004/12/03 12:37 577	2004/11/30 20:01:20 325 106 120		Y
				2004/12/01 07:31:46 000>198 834		
				2004/12/03 00:26:05 Halo 360 1216		
—	2004/12/02 ~0UT 348	1000 km/s N00W30	2004/12/03 02:48 577	2004/12/01 18:54:00 331 056 608	Same ICME as previous.	Y
				2004/12/03 00:26:05 Halo 360 1216		
153	2004/12/02 ~7UT 062	1800 km/s N30E30	2004/12/01 23:27 130	2004/12/03 00:26:05 Halo 360 1216	Same CME as following?	Y
154	2004/12/02 ~0UT 122	1000 km/s S15E05	2004/12/03 12:54 130	2004/12/03 00:26:05 Halo 360 1216	Same CME as previous?	Y
155	2004/12/16 ~8UT 119	1000 km/s S15E30	2004/12/16 12:29 –	2004/12/15 17:36:05 Halo 360 620	Halo early (but slow) and	W
				2004/12/16 04:24:05 138 024 725	nonhalo very narrow.	
156	2004/12/23 ~10UT 115	800 km/s S15E15	2004/12/25 09:46 580	2004/12/25 07:24:06 074 101 256		Y
157	2004/12/29 ~17UT 103	1800 km/s S00E90	2004/12/29 10:45 636	2004/12/29 07:45:06 103 024 305	Narrow CMEs	W
				2004/12/29 09:21:05 105 036 345		
158	2004/12/29 ~20UT 098	1200 km/s S30E30	2004/12/30 05:55 618	2004/12/29 09:21:05 105 036 345		Y
				2004/12/29 16:45:05 071 140 774		
159	2004/12/29 ~20UT 109	1400 km/s S75E30	2004/12/30 06:03 701	2004/12/30 10:57:06 072>176 1247		Y
160	2004/12/31 ~15UT 117	1200 km/s S30E05	2005/01/01 10:02 694	2004/12/31 17:06:05 277 116 293		Y
				2005/01/01 00:54:05 Halo 360 832		
				2005/01/02 09:06:05 102 035 271		
161	2005/01/03 ~2UT 118	1000 km/s S15E60	2005/01/03 06:44 517	2005/01/02 09:06:05 102 035 271		Y
				2005/01/03 05:30:05 093 124 389		
162	2005/01/05 ~18UT 125	1600 km/s S45E60	2005/01/05 17:46 600	2005/01/05 15:30:06 Halo 360 735	Same Halo.	Y
—	2005/01/06 ~2UT 141	1400 km/s S30E75	2005/01/05 22:27 366	2005/01/05 15:30:06 Halo 360 735	Same Halo.	Y
—	2005/01/06 ~0UT 122	1600 km/s S15E30	2005/01/06 15:27 366	2005/01/05 15:30:06 Halo 360 735	Same Halo.	Y
163	2005/01/09 ~11UT 097	1600 km/s S45E75	2005/01/09 17:55 580	2005/01/08 20:58:46 101 020 398		Y
				2005/01/09 09:06:05 094 164 870		
164	2005/01/11 ~7UT 112	2800 km/s S75E05	2005/01/09 06:40 249	2005/01/10 18:30:05 134 096 251		Y
165	2005/01/15 ~0UT 078	1200 km/s N30E01	2005/01/15 18:39 776	2005/01/15 06:30:05 Halo 360 2051	Same CME as following	Y
				2005/01/15 23:06:50 Halo 360 2861		
—	2005/01/17 ~4UT 320	2800 km/s N30W30	2005/01/17 08:51 500	2005/01/17 09:30:05 Halo 360 2094	Same CME as previous.	Y
				2005/01/17 09:54:05 Halo 360 2547		
166	2005/01/16 ~5UT 118	1800 km/s S15E45	2005/01/16 11:01 –	LASCO obscured	by snow storm	O
—	2005/01/16 ~11UT 122	2600 km/s S45E05	2005/01/16 08:00 –	Same ICME as previous.		O
167	2005/01/19 ~2UT 319	2200 km/s N45W30	2005/01/19 07:02 1137	2005/01/19 08:29:39 Halo 360 2020		Y
				2005/01/19 10:54:24 320 033 823		
168	2005/01/19 ~16UT 332	2000 km/s N15W30	2005/01/20 03:44 1280	2005/01/20 06:54:05 Halo 360 882		Y
169	2005/01/20 ~0UT 324	3600 km/s N15W75	2005/01/20 19:24 954	2005/01/20 17:06:55 309 018 799	Narrow CMEs.	O
				2005/01/20 23:18:05 292 031 728	LASCO obscured by snow storm.	

Table 1. (continued)

No.	SMEI Date Time PA	SMEI Speed Direction	Onset Time Point P Speed	LASCO Time PA Width Speed	Comments	?
				2005/01/20 04:58:50 295 022 551		
170	2005/01/20 ~13UT 128	800 km/s S30E30	2005/01/21 02:08 224	2005/01/20 06:54:05 Halo 360 882	Separate slow eruption?	Y
171	2005/01/27 ~0UT 188	2600 km/s S15W30	2005/01/27 03:39 –	No LASCO association.		N
172	2005/01/26 ~2UT 151	1200 km/s S15E05	2005/01/27 14:51 –	No LASCO association.		N
173	2005/01/26 ~22UT 004	1400 km/s N30E30	2005/01/25 00:05 –	No LASCO association.		N
174	2005/01/29 ~19UT 068	1400 km/s N00E75	2005/01/29 11:58 439	No LASCO association.		N
175	2005/02/01 ~4UT 130	2200 km/s S00E90	2005/01/31 01:00 689	2005/01/30 15:54:05 198 156 454		Y
				2005/01/31 07:31:44 152 220 1447		
176	2005/02/01 ~20UT 126	1400 km/s S15E30	2005/02/02 09:22 232	2005/02/02 04:06:06 172 093		Y
177	2005/02/14 ~5UT 353	1400 km/s N30W01	2005/02/14 15:35 –	No LASCO association.		N
178	2005/02/16 ~10UT 313	3000 km/s N00W30	2005/02/16 16:45 –	No LASCO association	Halo CME on 2005/02/17 too late.	N
179	2005/03/01 ~19UT 332	1200 km/s N75W30	2005/03/01 09:26 398	2005/02/28 22:30:06 190 228 503		Y
180	2005/03/02 ~3UT 014	1000 km/s N30E05	2005/03/02 20:18 636	2005/03/01 00:30:05 336 099 226		Y
181	2005/03/03 ~7UT 033	2400 km/s N45E05	2005/03/01 18:39 –	2005/03/01 19:31:45 303 073 609		Y
182	2005/04/20 ~10UT 027	2600 km/s N75E01	2005/04/19 06:37 192	2005/04/19 22:06:05 Halo 360 824	Not a halo. No component to north.	Y
—	2005/04/20 ~13UT 020	2000 km/s N15E60	2005/04/19 06:37 276	2005/04/18 10:06:05 022 037 309	Same ICME as previous.	W
183	2005/06/10 ~1UT 100	3200 km/s S45E05	2005/06/09 13:07 153	2005/06/09 17:00:06 070 094 461	Faint, but wide CME.	Y
184	2005/06/16 ~3UT 342	3000 km/s N75W05	2005/06/15 19:59 724	missing LASCO data	2005/06/16 16:05–2005/06/18 18:00	O
185	2005/06/14 ~23UT 320	2400 km/s N00W60	2005/06/14 15:05 153	2005/06/14 07:24:05 Halo 360 791		Y
—	2005/06/14 ~19UT 282	2000 km/s N00W90	2005/06/14 15:31 724	2005/06/14 16:00:05 289 073 —	Same ICME as previous.	Y
186	2005/06/18 ~16UT 052	1400 km/s N15E45	2005/06/18 06:03 184	2005/06/18 18:21:46 075 055 648		Y
187	2005/06/19 ~7UT 110	1000 km/s S15E01	2005/06/20 20:44 –	2005/06/19 02:36:05 103 087 324		Y
				2005/06/19 23:24:06 115 029 389		
188	2005/06/28 ~19UT 017	2800 km/s N60E75	2005/06/27 21:20 438	2005/06/28 17:06:05 Halo 360 1303		Y
189	2005/06/29 ~20UT 355	1800 km/s N15W75	2005/06/29 14:24 596	No LASCO association.		N
190	2005/07/06 ~20UT 128	3800 km/s S30E30	2005/07/05 23:40 –	2005/07/05 15:30:05 Halo 360 772		Y
191	2005/07/09 ~4UT 338	3400 km/s N30W60	2005/07/08 21:19 730	2005/07/07 17:06:07 Halo 360 683	Halo too early and faint.	W
192	2005/07/09 ~15UT 307	1800 km/s N00W30	2005/07/10 04:23 1099	2005/07/09 22:30:05 Halo 360 1540		Y
				2005/07/10 08:54:05 290>182 835		
193	2005/07/13 ~11UT 287	1600 km/s N60W45	2005/07/13 11:13 742	2005/07/13 03:06:05 288 054 759		Y
				2005/07/13 12:54:05 275 049 471		
				2005/07/13 14:30:05 Halo 360 1423		
194	2005/07/14 ~6UT 281	2600 km/s N60W75	2005/07/14 02:51 900	2005/07/14 06:30:05 282 060 541		Y
				2005/07/14 07:54:05 266 103 752		
				2005/07/14 10:54:05 Halo 360 2115		
195	2005/07/14 ~0UT 180	1000 km/s S15E05	2005/07/15 21:40 –	2005/07/15 21:08:02 253 174 820	faint component south	Y
196	2005/07/13 ~6UT 266	1000 km/s S00W15	2005/07/15 10:07 806	2005/07/14 10:54:05 Halo 360 2115		
				2005/07/14 17:54:05 278 054 703		
197	2005/07/30 ~14UT 038	3800 km/s N60E45	2005/07/29 21:44 489	2005/07/29 12:06:20 087 048 381		Y
				2005/07/30 06:50:28 Halo 360 1968		
198	2005/07/29 ~8UT 101	1400 km/s N30W05	2005/07/29 19:36 –	2005/07/28 22:06:20 081>213 1478		Y
				2005/07/30 00:54:37 107 025 205		
199	2005/08/03 ~2UT 325	1200 km/s N30W05	2005/08/04 00:29 562	No LASCO association.		N
200	2005/08/10 ~0UT 298	800 km/s N30W05	2005/08/11 08:52 328	2005/08/10 10:19:07 300 10		W
201	2005/08/17 ~11UT 105	2200 km/s S45E30	2005/08/15 16:46 –	2005/08/15 23:54:07 117 078 289	Faint narrow CME.	Y
202	2005/08/19 ~3UT 156	2200 km/s S15E30	2005/08/17 05:42 –	2005/08/19 12:54:05 115 060 246		Y
203	2005/08/20 ~21UT 082	3200 km/s N30E60	2005/08/19 02:52 141	2005/08/19 23:06:05 019>145 239		Y
				2005/08/20 05:58:33 054 057 027		
				2005/08/20 18:57:47 055 071 342		
				2005/08/20 21:30:08 020>157 420		

Table 1. (continued)

No.	SMEI Date Time PA	SMEI Speed Direction	Onset Time Point P Speed	LASCO Time PA Width Speed	Comments	?
204	2005/08/23 ~0UT 096	2000 km/s N15E01	2005/08/24 05:06 –	2005/08/23 03:06:07 075 074 738		Y
				2005/08/23 07:31:45 068 048 800		
				2005/08/23 14:54:05 Halo 360 1929		
205	2005/08/27 ~22UT 077	3800 km/s N00E60	2005/08/26 15:44 156	2005/08/26 03:30:05 072 023 281		Y
				2005/08/26 06:30:05 082 037 516		
				2005/08/26 08:54:05 072 056 448		
				2005/08/26 12:06:05 079 060 635		
206	2005/09/07 ~7UT 084	2200 km/s N00E30	2005/09/07 11:23 –	2005/09/07 05:48:06 085 074 195		Y
207	2005/09/09 ~20UT 120	3400 km/s S60E75	2005/09/09 11:59 777	2005/09/09 19:48:05 Halo 360 2257		Y

[a]The SMEI onset date and time are from the Cube-Fit and the PA is the position angle at which the elongations were made. The speed, latitude, longitude are the parameters from the Cube-Fit and the direction represents the quadrant in which the measurements were made. The following column shows the Point P speed for each event along with the linear fit onset time. The parameters for the associated LASCO event, are next followed by comments, and the final column is a classification on the suitability of a LASCO association: Y, yes; W, weak; N, No; and O, missing LASCO data.

LASCO speeds more accurately, with the range in each case being 200–400 km/s. This correlation is to be expected as both the LASCO and Point P case are projected speeds, hence the true speed is generally higher than those shown here. The Cube-Fit plots are much higher, with the speed >2000 km/s. While a generally higher speed distribution is expected upon the removal of projection effects this seems to be excessive. We note that the Cube-Fit procedure has been introduced as an alternative to the linear trend and is limited. This discussed further later in the paper.

[19] Physically, one may question the validity of an ICME that accelerates from the LASCO field-of-view and then decelerates again near 1 AU. While we are not necessarily defending the seemingly excessively large speeds from the Cube-Fit for some events, there is evidence from previous papers that suggests that many CMEs experience a secondary driving force once they leave the field-of-view of LASCO, that may continue well beyond 0.5 AU. Discussion on such a driving force is given by *Manoharan et al.* [2001], *Manoharan* [2006], and *Howard et al.* [2007].

4. Results

[20] A summary of our findings can be found in Table 1. The listed LASCO associations were identified using the same parameters listed in the CDAW LASCO CME Catalog [*Yashiro et al.*, 2004], i.e., date and time, central PA, PA width and sky plane projected speed. Many of our events are listed in this catalog. We have carefully examined the LASCO data for each SMEI event and as a result some LASCO events appear in Table 1 that are not in the catalog. The elongation range for each event (not shown here) is shown up to the end of 2004 in the corresponding table by *Webb et al.* [2006]. Similarly to the event discussed in section 3, we identified 143 events where there was a clear association between LASCO CME and SMEI ICME activity. In many cases there were several plausible LASCO events that could be associated with the SMEI event. Figure 4 shows elongation-time plots for two events (Events 171 and 172) in January 2005 where SMEI events were detected for which there were no LASCO associations. Both ICMEs were directed southward (PAs of 185° and 150°) and the linear onset times of each ICME were calculated at around 03:40 and 15:00 on 27 January respectively. The Cube-Fit onset times were around 00:00 on 27 January and 02:00 on 26 January. So, for the first event the selection search range is from 00:00 on 26 January to 15:40 on 27 January. During this time there was no LASCO activity at all in the quadrant covering PA range 140°–230°. For the second event the selection search range is from 02:00 on 25 January to 03:00 on 28 January. During this time no LASCO activity was detected in the 105°–195° quadrant. We cite these as examples where there are clear SMEI ICMEs not associated with anything in LASCO.

[21] Out of the 189 events observed by SMEI during the 32 month time interval of clear LASCO coverage, we identified 14 events that were not associated with LASCO activity at all, and a further 32 events with only weak activity, such as a faint, narrow and slow CME. There were also 18 SMEI ICMEs that had onset times near or during periods where LASCO was not taking data or the coronal images were ambiguous.

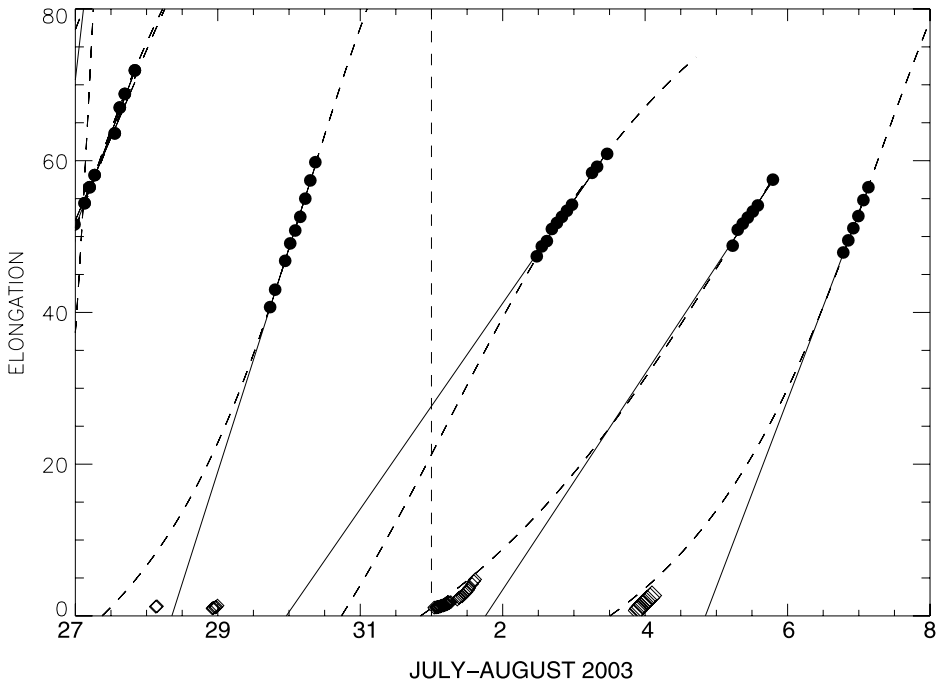

Figure 3. Elongation-time plots for a selected 12 d time period, from 27 July to 8 August 2003. The filled circles represent measurements from SMEI data while the open diamonds are measurements from LASCO. Small diamonds represent narrow CMEs (i.e., projected width $\leq 30°$). Plots are shown for the complete passage of 4 ICMEs while a fifth is also partially included on 27 July. Solid lines show the linear fit through the SMEI data while the dashed curve represents the Cube-Fit. The vertical dashed line represents the start of a new month, in this case August 2003. Of the four complete events, the former two are associated with very faint, slow and narrow and slow CMEs in LASCO, the latter of which occurs almost a day before the projected onset of the second ICME (on 30 July). The latter two events (on 5 and 6–7 August) are examples where there is a clear association with a CME in LASCO. In these two cases we believe the event observed by LASCO is the same as that observed by SMEI while the former two SMEI ICMEs require further explanation.

4.1. Weakly Associated Events

[22] Here we discuss an event for which we could only find a weak association with LASCO. Figure 5 shows LASCO C2 and SMEI running difference images for an event that occurred on 28–29 July, 2003. Its elongation-time plot, and that of another weakly associated event, are shown in Figure 3. Only 1 CME was found to be associated with this event (shown in Figure 5b), that was so faint, narrow ($\Delta W \sim 20°$) and slow (<200 km/s) that it is not recorded on the online CME catalogs. However, the SMEI images (shown in Figure 5a) show a bright (by SMEI standards), wide ($\Delta W > 30°$) and fast ($\sim$1000 km/s) ICME that is associated with no other LASCO CME. We identified 32 similar ICMEs (17% of those SMEI events with usable LASCO data), that were associated with either slow, faint CMEs, LASCO outflows that did not resemble CME eruptions or had their timing or location mismatched somewhat from the SMEI onset and propagation direction (e.g., if the associated CME occurred too late or was not in, but close to, the same quadrant as the SMEI ICME).

[23] If the LASCO CME is responsible for the SMEI ICME then something must have occurred to enhance its visibility, width and speed en-route through the interplanetary medium. The most plausible explanation is that the magnetic structure comprising the CME does not contain sufficient material to be easily detected by LASCO, and that it sweeps up solar wind material on transit that builds up in front of the CME. This solar wind material would effectively increase the mass of the CME, making it visible when it arrived in the field-of-view of SMEI. This is called the Snow-Plow Effect and the transient observed in white light would be due to swept up solar wind material and not coronal material from near the Sun. *Howard et al.* [2007] attempted to model the Snow-Plow Effect for two events and demonstrated that the total mass of the CME could almost double as a result of swept up solar wind material. Coupled to this, since the swept-up material is ionized, it may be concentrated near the leading edge of the moving magnetic structure, thereby enhancing its visibility. At this time we do not have a sufficiently accurate calibration of the SMEI data to enable us to derive the mass to a meaningful precision.

[24] For the event shown here the speed of the CME may pose limitations to the Snow-Plow effect. The speed as measured is far slower than the surrounding solar wind and so it may not be expected to be physically able to be effective at collecting solar wind material. Given the shape of the structure as observed by LASCO (Figure 5b) it is

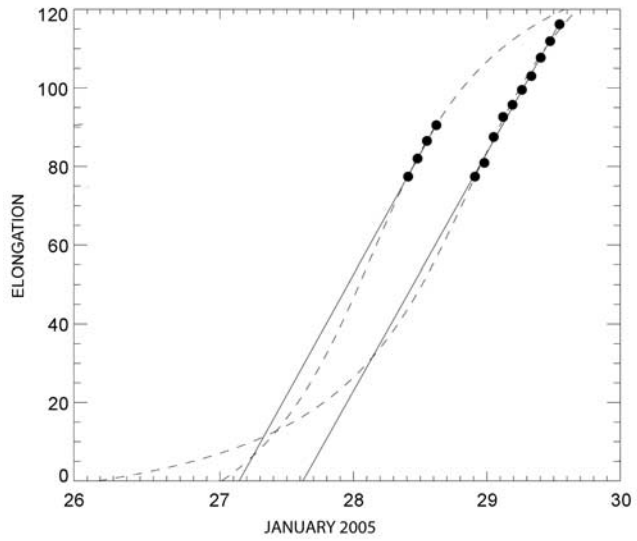

Figure 4. Elongation-time plots for two SMEI ICMEs that are not associated with LASCO CMEs. The onset times of these SMEI ICMEs are shown as the point where the curves intersect the time axis. These are from early 26 January 2005 to mid 27 January 2005, and no LASCO activity was observed for 24 h prior to, or 12 h after to the limits in these times in the same quadrant as each SMEI ICME.

conceivable that we are only observing one end of the CME and are hence measuring the speed of the CME flank rather than its leading edge. Hence we suggest that there is a faster component of this eruption to the east of the detected region that is invisible to LASCO.

[25] Alternatively we may disregard the LASCO event as being the source of the SMEI ICME. In this case each of the events we have classified as "W" (weak) would be reclassified as "N" (no association), increasing the number of unassociated events to 47. This represents 25% of the SMEI events that are associated with usable LASCO data sets. For most events a reasonable assessment would likely reclassify most of the "W" events as "N" but we have remained conservative in our approach here. In reality it is likely that some of the events we have classified as weakly associated are in fact associated with the SMEI ICME while others are unassociated. In the interests of impartiality we will leave as "W" any SMEI event where there is even a question of a LASCO association. Further and more detailed study of each of these events may assist in their reclassification.

4.2. Unassociated Events

[26] We now move to those SMEI ICMEs for which there is no association in LASCO. In each of these cases there is no LASCO transient activity of any kind near the time and quadrant of the projected ICME onset. Figure 4 shows an elongation-time plot for a SMEI ICME with no LASCO counterpart at all during the time period imposed by our selection criteria. We identified 14 such events and they are summarized in Table 2 (Figure 5).

[27] In the absence of LASCO activity, we applied the same selection criteria to solar X-ray, EUV and Hα data. That is, identify any evidence of activity around the right time and quadrant as the ICME onset. Using cataloged X-ray and Hα flare data and direct observation of EIT data we searched for phenomena known to be associated with CMEs, e.g., flares, erupting prominences, coronal dimming, etc. We have also noted the location of any nonpolar coronal holes with respect to the ICME location. Since coronal holes are regarded as the source for a fast-flowing solar wind stream, a coronal hole at low latitudes represents a corotating fast stream that may interact with its neighboring slower streams, resulting in a corotating interaction region.

Table 2. The 15 ICMEs not Associated With LASCO Activity and Associated Solar "Surface" Activity[a]

No.	SMEI Onset Date Time PA	EIT Coronal Hole	Hole?	Flare?	"Surface" Eruption
002	2003/02/10 ~8UT 232	NE and SE, nothing W	N	Y	X-ray flare C1.1 near N10W45.
030	2003/04/16 ~2UT 015	S, moves to the SW, nowhere near the north.	N	N	Faint eruption at 2003/04/15 03:36 near the NW limb moving N.
064	2003/07/24 ~18UT 309	Near disk center to N (S) and W (E).	W	N	Dimming at 2003/07/23 22:12 to NW.
065	2003/07/23 ~10UT 088	Same as above.	N	N	Eruption near NE pole on the limb which moves to near E equator.
129	2004/05/27 ~8UT 013	E-W band to N near equator near the NW	Y	N	Eruption/dimming at 2004/05/27 12:36 near disk center. Mostly S but some N.
130	2004/05/26 ~8UT 008	same as above	Y	N	No eruption.
171	2005/01/27 ~0UT 188	Two holes around 0–60 N and S starting E.	N	N	Faint eruption at 2005/01/27 03:34 to the SW extending from near equator to near limb.
172	2005/01/26 ~2UT 151	Same as above.	Y	N	No eruption.
173	2005/01/26 ~22UT 004	Same as above.	Y	N	No eruption.
174	2005/01/29 ~19UT 068	New hole emerges from E at around 45N.	W	N	No eruption.
177	2005/02/14 ~5UT 353	narrow hole around 30N to E	N	N	Large eruption at 2005/02/14 04:00 at around 45N near disk center. A later dimming.
178	2005/02/16 ~10UT 313	Same as above.	N	Y	Two eruptions at 2005/02/16 19:36 near disk center and then an X-ray flare at 23:30 from the same region.
189	2005/06/29 ~20UT 355	NE to disk center	W	N	No eruption.
199	2005/08/03 ~2UT 325	none apart from polar holes	N	Y	X-ray flare at 2003/08/03 20:54 near disk center. Also a faint eruption near the NW limb.

[a]Shown are the number and onset date and time of the ICME, as listed in Table 1. The coronal hole association for every event is given along with a rating of the likelihood of association with the ICME (Y, W, N). X-ray flare association is also indicated (Y, N) and finally, a summary of the associated eruptive phenomenon is given.

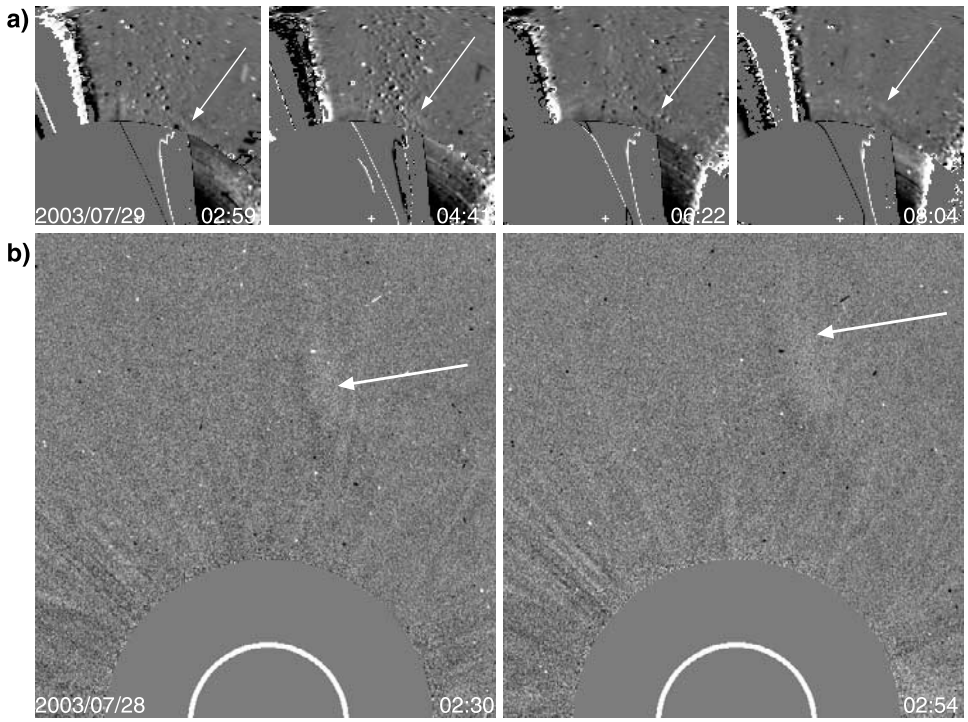

Figure 5. Running difference (i.e., with the previous image subtracted) (a) SMEI and (b) LASCO C2 images of a CME ICME event that occurred on 28–29 July, 2003. The solid grey quadrants obscuring the majority of the bottom half and left side of the SMEI images are data gaps, caused either by Camera 3 shutter closure or natural noise from auroral ovals, polar cap passage etc. The white "+" in the bottom-center of each SMEI image represents the location of the Sun. The white circle in the LASCO images represents the solar "surface" while the grey disk represents the occulting disk of the C2 instrument. The elongation-time plots for this event are shown in Figure 3. Only a single CME was found to be associated with this event, and it was faint, narrow ($\Delta W = 20^\circ$) and slow (<200 km/s). It occurred around 00:00 on 28 July and is shown in Panel (b). There is no other CME activity observed in LASCO in this quadrant. We classify this as a weakly associated event, as although we cannot exclusively rule out any LASCO association we also cannot conceive how such a CME can evolve to become the bright, wide ($\Delta W > 30^\circ$) and fast ($\sim$1000 km/s) ICME observed by SMEI.

This is discussed in the next section. Table 2 summarizes these observations. Of the 14 unassociated events, three were associated with X-ray flares (all C class), four were associated with a low latitude coronal hole, a further three were loosely associated with a low latitude coronal hole, and 10 were associated with an EUV eruption of some kind (including flares). Every event that was not associated with an eruption was associated to some extent with a coronal hole. It should be noted that for every event there were small EIT data gaps.

5. Discussion

[28] In order to regard the physical possibilities of the unassociated SMEI ICMEs, we must first account for possible instrumental or natural effects that may result in the inability to detect existing CMEs in LASCO. First, we have disregarded all events where LASCO data were unavailable, reducing our data set of SMEI ICMEs from 207 to 189 events. Second, we may disregard backsided events (i.e., CMEs with a trajectory behind the Sun relative to the Earth), as those undetected by LASCO would be much less likely to be observed in SMEI. Back-sided CMEs disperse in relative intensity much faster than front-sided CMEs because of their increasing distance from both the detector at Earth and the so-called "Thomson surface" [e.g., *Vourlidas and Howard*, 2006]. Hence if a back-sided CME is too faint to be detected by LASCO it will be even fainter by the time it arrives in the field-of-view of SMEI. To date, no back-sided ICME has been confirmed in SMEI data. Finally, we must consider whether Earth-directed, or halo CMEs very close to the Sun-Earth line may be responsible. It is possible that such CMEs may be sufficiently far from the Sun by the time their projection enters the field-of-view of LASCO that they escape detection [*Cliver et al.*, 1999]. The events unassociated with CMEs reported by *Tripathi et al.* [2004], for example, were close to solar disk center. Such transients may increase in relative brightness as they approach the Earth due their proximity to both the detector and "Thomson Sphere". We rule this out with the following arguments: First, as shown in Figure 1 a CME directed near the Sun-Earth line would arrive at 1 AU at elongation $\epsilon = 90^\circ$. Hence the ICME as detected by SMEI would be brightest near this elongation angle. Of the 14 unassociated SMEI events, six were detected around $\epsilon = 90^\circ$, four were measured up to around $\epsilon = 70^\circ$, while the remaining four

were at low elongations only ($\epsilon \leq 45°$). However, it must be stated that because the ICMEs are detected at $\epsilon = 90°$ does not mean they were Earth directed. Certainly, no brightening in SMEI occurred for any of these events.

[29] Second, if the ICME was directed along the Sun-Earth line there is a good chance a part of it would impact with the Earth, possibly causing a geomagnetic storm and passing an in situ spacecraft. For none of the unassociated ICMEs was an increase in geomagnetic activity recorded or a shock or magnetic cloud detected by the ACE spacecraft.

[30] Disregarding possible instrumental effects, we now consider the physical possibilities for the unassociated SMEI ICMEs. Regarding previous work done in this area, we offer the following possibilities.

[31] 1. The CME shock structure expands well beyond the structure observed in LASCO [*Howard*, 2006]. This may explain how some non-HCMEs may cross the Sun-Earth line en-route to be detected near the Earth but it is difficult to reconcile how such an expansion could occur across an entire quadrant of the sky, where no LASCO activity was apparent.

[32] 2. The CME corotates with the Sun, such that its projection in the sky varies according to the rate of solar rotation [*Howard*, 2006]. This would require CMEs to be rigidly fixed to the Sun and to move independently of the solar wind, which seems to be physically implausible.

[33] 3. CMEs have an as yet uninvestigated nonradial expansion that changes their projected geometry as they move into the interplanetary medium [*Howard*, 2006]. Investigation of this possibility is impossible given the data used in the present study.

[34] 4. Bright transients observed in SMEI are not due to ICMEs at all, but rather the sweeping past the SMEI cameras of a large, dense region such as the heliospheric current sheet (*R. A. Howard*, private communication, 2006). This phenomenon may have been observed in Helios data [*Leinert et al.*, 1975]. If this were the case the movement of the transient would be expected to have very low speeds, and the direction (away from and toward the Sun) would vary from event to event. This is not observed in SMEI data, where transients are generally fast and always antisunward.

[35] 5. ICMEs are caused by solar wind material driven by shocks from corotating interaction regions. This has been suggested to be the case for a small number of earth-directed ICMEs [*Howard and Tappin*, 2005b].

[36] 6. ICMEs are caused by solar wind material driven by shocks from blast waves of flares [e.g., *Shanmugaraju et al.*, 2006, and references therein].

[37] 7. The CME is invisible to LASCO because it does not contain sufficient matter for its intensity to be brighter than the detection threshold of the instrument [*Simnett*, 2005]. *Howard and Tappin* [2005b] used the term EMS (or Erupting Magnetic Structures) to describe these eruptions, following the terminology of *Lyons and Simnett* [2001]. It must be noted that the EMS terminology used by *Lyons and Simnett* [2001] describes a slightly different phenomenom to that discussed here. It has been decided to use this terminology to describe these events to remain consistent with more recent papers that have adopted this terminology [e.g., *Simnett*, 2005; *Howard and Tappin*, 2005b].

[38] Reducing this list to only those that are most likely, we have corotating interaction regions and erupting magnetic structures. Each is discussed in the following sections.

5.1. Corotating Interaction Regions

[39] Corotating Interaction Regions (CIRs) [*Smith and Wolfe*, 1976] occur when fast solar wind, typically from coronal holes, interacts with slow solar wind due to corotation at low latitudes, causing a region of compression. They are bound by forward and reverse waves that may form forward and reverse shocks, typically beyond 2 AU. The possibility of CIRs as the source of ICMEs unassociated with CMEs has been investigated by *Howard and Tappin* [2005b], and direct imaging of CIRs has been made using Helios data [e.g., *Webb and Jackson*, 1990].

[40] To determine whether the unassociated SMEI ICMEs are due to CIRs we must assign identification criteria based on the available data. Signatures of CIRs are well documented with in situ data [e.g., *Pizzo*, 1978, 1980] but we do not have such reliable data for the ICMEs identified in the present study. This is because CIRs rarely form shocks within 1 AU and so a clear signature in the in situ spacecraft cannot be identified. Upon examination of ACE SWEPAM and EPAM data we could not identify any such CIR signature. We are thus limited only to observational evidence using solar images. As CIRs are due to fast flowing solar wind interacting with slower solar wind, and coronal holes are sources of fast solar wind, coronal holes may be regarded as a part of the source of a CIR [e.g., *Krieger et al.*, 1973]. In order to experience sufficiently strong corotation these would need to be near the solar equator.

[41] We may also speculate on the appearance of a CIR with respect to the SMEI cameras. First, assuming none of the unassociated ICMEs are Earth directed, we may disregard coronal holes that are nearer the pole than the equator. This is because the near polar solar wind does not experience sufficient corotation to cause a strong interaction region. Second, we may disregard events that appear to be fast moving, as the interface between the flowing streams would not be expected to move with great speed. Third, we may disregard events that are moving in the western direction, as the relative geometry of the CIR at elongations below around 120° results in the transient appearing only in the eastern sector of the sky and moving slowly outward, or eastward [*Tappin*, 1987]. According to *Tappin* [1987], once the observed part of the CIR transient reaches 120° elongation the Earth is imbedded within the transient, so at this point it would also appear in the western sector of the sky. Given that the vast majority of the SMEI ICMEs, including all of the unassociated events were observed at $\epsilon < 120°$, this unlikely explanation has been disregarded.

[42] Table 2 shows information on the coronal hole activity associated with each unassociated SMEI ICME. Of the 14 events there are four that are labeled "Y" and a further three labeled "W". These represent coronal holes that are well associated and weakly associated with the region of the ICME around the time of its onset. Of these seven events, only two (Events 64 and 174) are associated with ICMEs with a span within 45° of the equator. Of these, only Event 174 is in the eastern hemisphere and moving eastward. This event is also not associated with any visible eruption in EUV or X-ray images. Hence it is conceivable

that this, and only this event, may be the result of a CIR. This leaves 13 ICMEs unaccounted for.

5.2. Erupting Magnetic Structures

[43] The remaining possibility is that which has become known as Erupting Magnetic Structures, or EMS [*Simnett*, 2005; *Howard and Tappin*, 2005b]. The physics behind these eruptions are the same as for a typical CME, that is they comprise a magnetic structure that erupts and moves away from the Sun with high speed [*Low*, 1996]. The difference is that these structures do not contain sufficient excess plasma over ambient to be detected by the coronagraphs. This is because coronagraphs measure light scattered from the electrons in plasma embedded in the CME structure. We have also offered this as the most plausible explanation for the weakly associated events discussed in section 4.1. In many of those cases the LASCO CME is detectable, but is very faint and often only part of the structure is visible.

[44] To test the possibility of EMS we must identify a way of detecting CMEs without the use of coronagraph data. We may attempt this by searching for phenomena known to be associated with CMEs. These include flares, erupting prominences/filaments, coronal dimming and coronal loop disconnection. We have searched for evidence of these around the onset time and location of each of the 14 unassociated events, and the results are shown in Table 2. There were 10 events that were associated with an eruption of some kind in EIT, while four were not associated with any solar activity in the right place and time.

[45] To account for the four events with no detected eruption we offer that every EIT database had data gaps during, for example, periods of time when the instrument cycles through its range of wavelength observations. It is possible that an eruption may have been missed during these times. Also it is known that many CMEs are not associated with solar activity. For example, *Howard et al.* [2008] conducted a study of 10512 cataloged CMEs and found that only 1961, or 19% were associated with X-ray or Hα flares, or disappearing Hα filaments. Of the 254 shocks associated with HCMEs studied by *Howard and Tappin* [2005a], only 102, or 40% were associated with M or X Class X-ray flares. We must also not disregard the possibility that there is an as yet undiscovered phenomena responsible for the unassociated SMEI ICMEs.

5.3. Flare Blast Waves

[46] It is worth explaining why we have rejected flare blast waves as the cause of the SMEI events. CMEs were originally thought of by some as resulting from an explosive release of energy in a flare. However, this would require the flare to cause the CME and for the initiating flare to be approximately near the center of the eruption. Detailed timing and location studies of CMEs with their associated flares were inconsistent with this idea [e.g., *Harrison and Sime*, 1989] and later theoretical work [e.g., *Low*, 1996] gave a much more plausible physical explanation of the CME phenomenon. We also note here that CMEs are present throughout solar minimum, when flares are largely absent.

[47] However, as a check we have searched for soft X-ray flares that had a class of B or higher and looked at all flares that were within 12 h of either the linear or Cube-Fit onset times. They were required to be in the same quadrant as the ICME observed by SMEI. Flare location was determined where possible using GOES SXI and associated Hα flare data, and where these data were not available we examined the location of the EUV component of the flare using EIT 195 Å data. Table 2 summarizes our findings. Of the 14 unassociated events only 3 were associated with an X-ray flare and none of the flares exceeded an emission peak greater than class C. Our conclusion is that there were no major candidate flares within the onset time window for the LASCO-unassociated SMEI events, and that we can therefore discount flare blast waves as their source.

5.4. Uncertainties and Limitations

[48] Identifying the appropriate CME(s) to be associated with the ICMEs observed in SMEI was the largest source of uncertainty in the present study for the following reasons.

[49] 1. Assigning a linear trend through elongation-time curves is unphysical. This is demonstrated in Figure 1.

[50] 2. The Cube-Fit curve was based on the assumption of constant speed ICMEs. ICMEs are generally expected to vary in speed as they move through the interplanetary medium due to their interaction with the surrounding solar wind. The possibility of adding a new dimension to the Cube allowing for accelerating and decelerating ICMEs was investigated, but the time required to run this procedure for all events was prohibitive.

[51] 3. We have not considered the possible effects of interacting CMEs.

[52] 4. As the SMEI ICME approaches 90° elongation we may expect to measure different parts of the ICME due to the change in relative brightness resulting from the geometry of lines of sight and Thomson scattering physics. We have not taken these affects into consideration and so may regard measurements from events with higher elongations with more suspicion than those at lower elongations.

[53] Considering these limitations we remain optimistic that the selection criteria we have devised is appropriate (given the generous time range for the selection criteria), and we have deliberately left the Cube-Fit routine as completely automated to remove possible bias toward LASCO events. While some of the specific CME associations with the SMEI events may be challenged, we are confident that the unassociated events discussed in this paper are undisputed.

6. Conclusions

[54] The identification of ICMEs without a CME counterpart has been a topic of some discussion and debate over the years. In the present paper we have identified a number of these events using SMEI, ranging from those ICMEs associated with only faint, slow, narrow and/or untimely LASCO transient activity to those with no associated LASCO counterpart at all. Out of the 189 SMEI ICMEs detected from 2003–2005 not associated with missing or unusable LASCO data, 32 were found to have a weak association in LASCO and a further 14 had no association at all. This represents a subset of 7–25% of the ICMEs identified by SMEI. Further investigation revealed that of the probable physical explanations for these events, corotat-

ing interaction regions accounted for one possible event while flare blast waves appeared unlikely. We suggest that the most likely explanation is erupting magnetic structures, that involves identical physics to a typical CME, except that the structure does not contain sufficient mass to be detected by coronagraphs.

[55] **Acknowledgments.** SMEI was designed and constructed by a team of scientists and engineers from the US Air Force Research Laboratory, the University of California at San Diego, Boston College, Boston University, and the University of Birmingham in the United Kingdom. SOHO is a project of international cooperation between ESA and NASA. This work was supported in part by NASA grant NNGO5GF98G and by the National Research Council Research Fellowship Program. The latter is funded by AFOSR contract F49620-02C-0015. We thank D. F. Webb, J. C. Johnston, and S. J. Tappin for helpful discussions, and T. A. Kuchar for his assistance in the production of the SMEI images.

[56] Amitava Bhattacharjee thanks Seiji Yashiro and another reviewer for their assistance in evaluating this paper.

References

Brueckner, G. E., et al. (1995), The large angle spectroscopic coronagraph, *Sol. Phys.*, *162*, 357.

Cane, H. V., and I. G. Richardson (2003), Interplanetary coronal mass ejections in the near-Earth solar wind during 1996–2002, *J. Geophys. Res.*, *108*(A4), 1156, doi:10.1029/2002JA009817.

Cliver, E. W., D. F. Webb, and R. A. Howard (1999), On the origin of solar metric type II bursts, *Sol. Phys.*, *187*, 89.

Delaboudinière, J.-P., et al. (1995), EIT: Extreme-ultraviolet imaging telescope for the SOHO mission, *Sol. Phys.*, *162*, 291.

Eyles, C. J., G. M. Simnett, M. P. Cooke, B. V. Jackson, A. Buffington, N. R. Waltham, J. M. King, P. A. Anderson, and P. E. Holladay (2003), The solar mass ejection imager (SMEI), *Sol. Phys.*, *217*, 319.

Harrison, R. A., and D. G. Sime (1989), The launch of coronal mass ejections: White light and X-ray observations in the low corona, *J. Geophys. Res.*, *94*, 2333.

Hewish, A., P. F. Scott, and D. Wills (1964), Interplanetary scintillation of small diameter radio sources, *Nature*, *203*, 1214.

Howard, T. A. (2006), Reply to comment by N. Gopalswamy et al. on "Interplanetary shocks unassociated with earthbound coronal mass ejections", *Geophys. Res. Lett.*, *33*, L11109, doi:10.1029/2005GL025233.

Howard, T. A., and S. J. Tappin (2005a), Statistical survey of earthbound interplanetary shocks, associated coronal mass ejections and their space weather consequences, *Astron. Astrophys.*, *440*, 373.

Howard, T. A., and S. J. Tappin (2005b), Earthbound interplanetary shocks unassociated with halo coronal mass ejections, *Geophys. Res. Lett.*, *32*, L14106, doi:10.1029/2005GL023056.

Howard, R. A., D. J. Michels, N. R. Sheeley Jr., and M. J. Koomen (1982), The observation of a coronal transient directed at Earth, *Astrophys. J.*, *263*, L101.

Howard, T. A., D. F. Webb, S. J. Tappin, D. R. Mizuno, and J. C. Johnston (2006), Tracking halo coronal mass ejections from 0–1 AU and space weather forecasting using the Solar Mass Ejection Imager (SMEI), *J. Geophys. Res.*, *111*, A04105, doi:10.1029/2005JA011349.

Howard, T. A., C. D. Fry, J. C. Johnston, and D. F. Webb (2007), On the evolution of coronal mass ejections in the interplanetary medium, *Astrophys. J.*, *667*, 610.

Howard, T. A., D. Nandy, and A. C. Koepke (2008), The kinematic properties of solar coronal mass ejections: Correction for projection effects in spacecraft coronagraph measurements, *J. Geophys. Res.*, *113*, A01104, doi:10.1029/2007JA012500.

Jackson, B. V., et al. (2004), The Solar Mass-Ejection Imager (SMEI) Mission, *Sol. Phys.*, *225*, 177.

Jackson, B. V., A. Buffington, P. P. Hick, X. Wang, and D. F. Webb (2006), Preliminary three-dimensional analysis of the heliospheric response to the 28 October 2003 CME using SMEI white-light observations, *J. Geophys. Res.*, *111*, A09S91, doi:10.1029/2004JA010942.

Krieger, A. S., A. F. Timothy, and E. C. Roelof (1973), A coronal hole and its identification as the source of a high velocity solar wind stream, *Sol. Phys.*, *29*, 505.

Leighly, J. B. (1955), Aitoff and Hammer: An attempt at clarification, *Geogr. Rev.*, *45*, 246.

Leinert, C., H. Link, E. Pitz, N. Salm, and D. Knuppelberg (1975), The Helios zodiacal light experiment (E9), *Raumfahartforschung*, *19*, 264.

Low, B.-C. (1996), Solar activity and the corona, *Sol. Phys.*, *167*, 217.

Lyons, M. A., and G. M. Simnett (2001), Erupting magnetic structures observed with SOHO/LASCO, *Sol. Phys.*, *200*, 203.

Manoharan, P. K. (2006), Evolution of coronal mass ejections in the inner heliosphere: A study using white-light and scintillation images, *Sol. Phys.*, *235*, 345.

Manoharan, P. K., M. Tokumaru, M. Pick, P. Subramanian, F. M. Ipavich, K. Schenk, M. L. Kaiser, R. P. Lepping, and A. Vourlidas (2001), Coronal mass ejection of 2000 July 14 event: Imaging from near-Sun to Earth environment, *Astrophys. J.*, *559*, 1180.

Pizzo, V. (1978), A three-dimensional model of corotating streams in the solar wind: 1. Theoretical foundations, *J. Geophys. Res.*, *83*, 5563.

Pizzo, V. (1980), A three-dimensional model of corotating streams in the solar wind: 2. Hydrodynamic streams, *J. Geophys. Res.*, *85*, 727.

Schwenn, R., A. Dal Lago, E. Huttunen, and W. D. Gonzalez (2005), The association of coronal mass ejections with their effects near the Earth, *Ann. Geophys.*, *23*, 1033.

Shanmugaraju, A., Y.-J. Moon, K.-S. Cho, M. Dryer, and S. Umpathy (2006), Origin of coronal shocks without mass ejections, *Sol. Phys.*, *233*, 117.

Simnett, G. M. (2005), CMEs observed by SMEI which are not seen by LASCO, in *Proc. Sol. Wind 11/SOHO 16 "Connecting Sun and Heliosphere"*, edited by B. Fleck and T. H. Zurbuchen, p. 767, ESA SP-592, ESTEC, Noordwijk, Netherlands.

Smith, E. J., and J. H. Wolfe (1976), Observations of interaction regions and corotating shocks between one and five AU-Pioneers 10 and 11, *Geophys. Res. Lett.*, *3*, 137.

St. Cyr, O. C., et al. (2000), Properties of coronal mass ejections: SOHO LASCO observations from January 1996 to June 1998, *J. Geophys. Res.*, *105*, 18,169.

Tappin, S. J. (1987), Numerical modelling of scintillation variations from interplanetary disturbances, *Planet. Space Sci.*, *35*, 271.

Tappin, S. J. (2006), The deceleration of an interplanetary transient from the Sun to 5 AU, *Sol. Phys.*, *233*, 233.

Tappin, S. J., et al. (2004), Tracking a major interplanetary disturbance with SMEI, *Geophys. Res. Lett.*, *31*, L02802, doi:10.1029/2003GL018766.

Tripathi, D., V. Bothmer, and H. Cremades (2004), The basic characteristics of EUV post-eruptive arcades and their role as tracers of coronal mass ejection source regions, *Astron. Astrophys.*, *422*, 337.

Vourlidas, V., and R. A. Howard (2006), The proper treatment of coronal mass ejection brightness: A new methodology and implications for observations, *Astrophys. J.*, *642*, 1216.

Webb, D. F., and B. V. Jackson (1990), The identification and characteristics of solar mass ejections observed in the heliosphere by the HELIOS 2 photometers, *J. Geophys. Res.*, *95*, 20,641.

Webb, D. F., et al. (2006), Solar Mass Ejection Imager (SMEI) observations of CMEs in the heliosphere, *J. Geophys. Res.*, *111*, A12101, doi:10.1029/2006JA011655.

Wild, J. P., S. F. Smerd, and A. A. Weiss (1963), Solar radio bursts, *Ann. Rev. Astron. Astrophys.*, *1*, 291.

Yashiro, S., N. Gopalswamy, G. Michalek, O. C. St. Cyr, S. P. Plunkett, and R. A. Howard (2004), A catalog of white light coronal mass ejections observed by the SOHO spacecraft, *J. Geophys. Res.*, *109*, A07105, doi:10.1029/2003JA010282.

Zhao, X.-P. (1992), Interaction of fast steady flow with slow transient flow - A new cause of shock pair and interplanetary B(z) event, *J. Geophys. Res.*, *97*, 15,051.

T. A. Howard, Air Force Research Laboratory, Space Vehicles Directorate, National Solar Observatory, P.O. Box 62 Sunspot, NM 88349, USA. (thoward@nso.edu)

G. M. Simnett, School of Physics and Astronomy, University of Birmingham, Edgbaston, B15 2TT, UK.